Optimal Triangular Mesh Generation By Coordinate Transformation

E.F. D'Azevedo
Department of Computer Science
University of Waterloo
Research Report CS-89-11

April, 1989

OPTIMAL TRIANGULAR MESH GENERATION BY COORDINATE TRANSFORMATION

E. F. D'AZEVEDO *

Abstract. This paper presents the motivation and construction of coordinate transformations that generate optimally efficient meshes for linear interpolation. The coordinate transformations are derived from a result in differential geometry in the characterization of a "flat" space. The optimality results are demonstrated for some numerical examples. Adaptive meshes produced by PLTMG are included for comparison. The paper concludes that coordinate transformation is a promising strategy for investigation into more complex optimal meshing problems in finite element analysis.

Key Words. Optimal triangular mesh, function interpolation, coordinate transformation

1. Introduction. The novelty of this paper is in the construction and demonstration of coordinate transformations that generate optimally efficient meshes for linear interpolation.

Consider the problem of interpolating a function with piecewise linear patches over a domain to within a given error tolerance. A triangular mesh that achieves this error tolerance with the *fewest* number of triangles is defined to be optimally efficient. The goal of this paper is the computation of an optimally efficient mesh where we assume the error tolerance is small and the influence of domain shape on triangulation is insignificant.

This paper is a basic study on optimal meshes with the intention of providing insight into the more complex meshing problems in finite element analysis. The engineering community is interested in finding optimal meshes under the criterion of minimizing the error in energy norm of variation problems in finite element analysis [14]. Some attempt have been the application of mathematical programming to find an optimal placement of mesh nodes, however such schemes are computationally expensive and typically encounter problems in mesh entanglement [4,6,7]. Others have applied effective heuristics in the generation of near optimal meshes [5,8,9,10,13,15]. This paper presents the approach of coordinate transformation of a regular mesh as a promising strategy for optimal mesh generation.

Coordinate transformation, especially conformal mappings obtained by the solution of Laplace's equation, is a technique in the generation of boundary-conforming curvilinear coordinate systems in finite difference solution of fluid dynamics. One aim of this transformation is to map a rectangular grid to fit the computation domain, maybe an aircraft wing, with some prescribed boundary conditions. Thompson [18,19,20] contain an extensive treatment on this subject. The coordinate transformation described in this paper is *not* determined by geometric considerations but derived from error properties in approximation.

* Department of Computer Science, University of Waterloo, Waterloo, Onatrio, Canada N2L 3G1, efdazevedo@watfun.uwaterloo.ca. This work was supported by the National Sciences and Engineering Research Council of Canada and by the Information Technology Research Center, which is funded by the Province of Ontario.

Nadler [11] and the author [2] have studied local coordinate transformation for generation of optimally efficient meshes. Peraire et al. [12] applied such local coordinate transformation in mesh generation for dynamic remeshing in solving compressible flow computations. In these works, piecewise linear approximation of a quadratic function is used as the model for local analysis. This paper extends the local results on optimally efficient meshes to apply *globally* for a class of functions, which includes harmonic and quadratic functions. In the following discussion, we focus our attention on the approximation of harmonic functions.

An outline of the paper follows. In Section 2, we derive the linear transformation that maps a regular mesh into an optimal mesh for the interpolation of a quadratic function. The transformation is suggested by the simplification of the exact error expression. In Section 3, this simplification of the local error expression motivates the extension of the coordinate transformation for optimal mesh generation to a wider class of functions. To state the condition for finding such transformations, we invoke a basic result in differential geometry for the characterization of a "flat" space. The condition can be shown by direct consideration of the integrability of some differential equations. We show that these transformations can be computed as the solution to a system of ordinary differential equations posed as an initial value problem. Section 4 contains discussions and error profiles of numerical experiments in the interpolation of harmonic functions. The results show remarkable agreement with the theoretical predictions. Experimental results for the meshes generated by PLTMG, a PDE solver with adaptive mesh refinement, in solving Laplace's equation with Dirichlet boundary conditions are included for comparison. The error profiles show the optimality of the triangulation, and also provide a measure of the efficiency of the adaptively generated mesh. Finally, in Section 5 we state our conclusion and suggest directions for further research.

2. Local Analysis by Quadratic Model. In this section, we show how a linear transformation of a regular mesh of optimal shape triangles yields an optimally efficient mesh for interpolating a quadratic function.

Let $E(x,y)$ be the error function obtained in the interpolation of a quadratic function

$$f(x,y) = (x,y)H(x,y)^t + d_1x + d_2y + d_3$$

over a triangle T. By definition, the error function $E(x,y)$ is a quadratic function and its level curves form a family of conics with a common center. It is a family of ellipses if $\det(H) > 0$, and a family of hyperbolae if $\det(H) < 0$. Let the center be at (x_c, y_c). The error at a displacement from the center is given by

$$E(x_c + dx, y_c + dy) = \mathcal{E} - (dx, dy)H(dx, dy)^t \tag{1}$$

where $\mathcal{E} = E(x_c, y_c)$. The derivation of (1) is by straight forward algebraic manipulation and the details are contained in Appendix A.

We see that if the symmetric matrix H is diagonalizable as

$$H = Q^t \begin{pmatrix} \lambda_1 & 0 \\ 0 & \lambda_2 \end{pmatrix} Q = R^t \begin{pmatrix} 1 & 0 \\ 0 & \epsilon \end{pmatrix} R \tag{2}$$

where

$$R = \begin{pmatrix} \sqrt{|\lambda_1|} & 0 \\ 0 & \sqrt{|\lambda_2|} \end{pmatrix} Q \quad , \quad \epsilon = sign(\det(H)) \tag{3}$$

then with $(d\tilde{x}, d\tilde{y})^t = R(dx, dy)^t$, the expression $(dx, dy)H(dx, dy)^t$ reduces to $(d\tilde{x})^2 + \epsilon(d\tilde{y})^2$. The error function can be rewritten as

$$\begin{aligned} E(x_c + dx, y_c + dy) &= \mathcal{E} - (dx, dy)H(dx, dy)^t \\ &= \mathcal{E} - ((d\tilde{x})^2 + \epsilon(d\tilde{y})^2) \\ &= \tilde{E}(\tilde{x}_c + d\tilde{x}, \tilde{y}_c + d\tilde{y}) \end{aligned}$$

where $\tilde{E}(\tilde{x}, \tilde{y})$ denotes the corresponding error function under transformation R.

In the following, we shall determine the best triangle shape for approximation. Consider first the case where $f(x, y)$ is convex shape, then the level curves or contours of $\tilde{E}(\tilde{x}, \tilde{y})$ are concentric circles given by

$$\tilde{E}(\tilde{x}_c + d\tilde{x}, \tilde{y}_c + d\tilde{y}) = \mathcal{E} - ((d\tilde{x})^2 + (d\tilde{y})^2)$$

Let $\tilde{T}$ be the transformed image of triangle T with vertices at $(\tilde{x}_1, \tilde{y}_1)$, $(\tilde{x}_2, \tilde{y}_2)$ and $(\tilde{x}_3, \tilde{y}_3)$. The circumcircle of $\tilde{T}$ corresponds to the level curve of value zero. Hence the radius of this circumcircle is $sqrt(|\mathcal{E}|)$ and relates directly to the maximum error attainable. We can easily see that an equilateral triangle covers the most area for a fixed circumcircle; therefore an equilateral triangle is of optimal shape.

Consider next the case where $f(x, y)$ is not convex but of a saddle shape, then we have

$$\begin{aligned} \tilde{E}(\tilde{x}, \tilde{y}) &= \tilde{E}(\tilde{x}_c + d\tilde{x}, \tilde{y}_c + d\tilde{y}) \\ &= \mathcal{E} - ((d\tilde{x})^2 - (d\tilde{y})^2) \\ &= \mathcal{E} - ((\tilde{x} - \tilde{x}_c)^2 - (\tilde{y} - \tilde{y}_c)^2) \end{aligned}$$

We note that the error function $\tilde{E}(\tilde{x}, \tilde{y})$ is a harmonic function and attains its extrema on the boundary of $\tilde{T}$. By calculus, we can show that the local extrema along edge $(\tilde{x}_i, \tilde{y}_i)$, $(\tilde{x}_j, \tilde{y}_j)$ is attained at the midpoint with value

$$\tilde{E}(\frac{\tilde{x}_i + \tilde{x}_j}{2}, \frac{\tilde{y}_i + \tilde{y}_j}{2}) = \frac{1}{4}|(\tilde{x}_i - \tilde{x}_j)^2 - (\tilde{y}_i - \tilde{y}_j)^2|$$

Thus the maximum error attained is

$$\frac{1}{4} \max |(\tilde{x}_i - \tilde{x}_j)^2 - (\tilde{y}_i - \tilde{y}_j)^2|$$

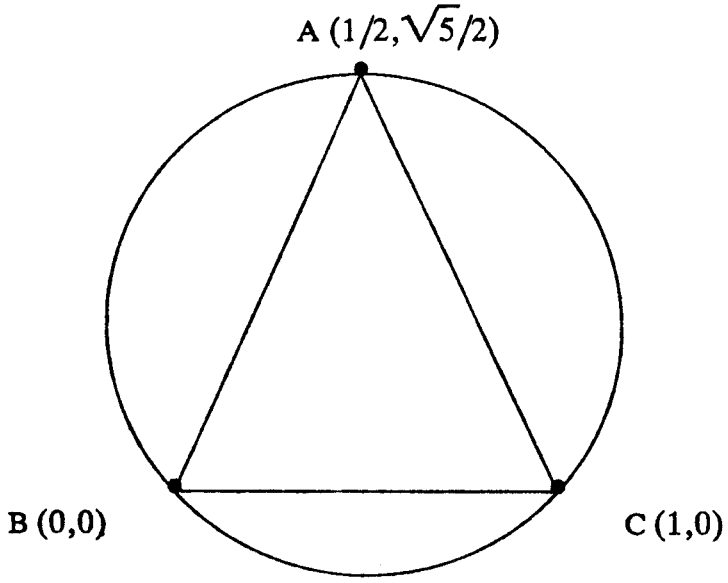

FIG. 1. *Optimal triangle geometry for saddle shape function*

The details in finding the optimal shape triangle is found in Appendix B. The optimal shape triangle geometry in this case is not unique and attains the same error on all three edges. Figure 1 shows an optimal shape triangle geometry chosen for the saddle shape functions.

Applying the results on optimal shape triangles, we see that a regular mesh of optimal shape triangles over the transformed plane corresponds to an optimally efficient mesh. Every triangle attains the same maximum error; moreover, these triangles cover the most area for the error attained and so are optimally efficient. Since the transformation R in (3) is basically a rotation followed by a rescaling of coordinate axes, we find the areas of triangles are scaled accordingly. Hence the inverse transformation R^{-1}, maps this regular mesh to produce an optimally efficient mesh in the original plane.

3. Coordinate Transformation. Now locally, a function behaves as a quadratic given by its Taylor expansion

$$f(x+dx, y+dy) \approx \frac{1}{2}(dx,dy)H(dx,dy)^t + (dx,dy)\nabla f(x,y) + f(x,y)$$

where H is the hessian matrix at (x,y). Hence we can define local coordinate transformations for generation of optimally efficient meshes. The main goal of this section is to investigate into the extension of these local results to a wider class of functions.

3.1. Generalized Equidistribution. Mesh generation by equidistribution in one-dimensional problems can also be viewed as optimal mesh generation by coordinate transformation. Consider again the problem of linear interpolation of a quadratic function over an interval $[a,b]$. Let the error function be represented as,

$$E(x) = (x-a)(x-b)f_2$$

By calculus, $E(x)$ achieves a local extremum at $x_c = (a+b)/2$.

$$\begin{aligned} E(x_c+dx) &= ((x_c+dx)-a)((x_c+dx)-b)f_2 \\ &= ((x_c-a)+dx)((x_c-b)+dx)f_2 \\ &= (x_c-a)(x_c-b)f_2 + ((x_c-a)+(x_c-b))\,dx\,f_2 + (dx)^2 f_2 \\ &= E(x_c) + (dx)^2 f_2 \\ &= E(x_c) + \epsilon d\tilde{x}^2 \quad \text{where} \quad d\tilde{x} = dx\sqrt{|f_2|}\ , \ \epsilon = sign(f_2) \end{aligned}$$

By extension of local analysis, we require the coordinate transformation $\tilde{x}(x)$ such that,

$$d\tilde{x} = \sqrt{\frac{|f''(x)|}{2}}dx \tag{4}$$

One choice for $\tilde{x}(x)$ is

$$\tilde{x}(x) = \frac{1}{\sqrt{2}}\int_{x_0}^{x} \sqrt{|f''(t)|}dt \quad + C$$

Ideally, a uniform mesh in $\tilde{x}$-coordinate will yield an optimal mesh in the original coordinate space. Then the mesh nodes $\{x_i\}$ are obtained by equidistribution of $\sqrt{|f''(x)|}$, which is suggested by de Boor[3].

$$\begin{aligned}
\text{constant} &= \tilde{x}_{i+1} - \tilde{x}_i \\
&= \left(\frac{1}{\sqrt{2}}\int_{x_0}^{x_{i+1}} \sqrt{|f''(t)|}dt \quad + C\right) - \left(\frac{1}{\sqrt{2}}\int_{x_0}^{x_i} \sqrt{|f''(t)|}dt \quad + C\right) \\
&= \frac{1}{\sqrt{2}}\int_{x_i}^{x_{i+1}} \sqrt{|f''(t)|}dt
\end{aligned}$$

Therefore optimal triangular mesh generation by coordinate transformation can be viewed as a generalization of the techniques of equidistribution from one-dimension. White [21] has developed coordinate transformation to map uniform meshes to equidistributing meshes for solving two-point boundary value problems.

The generalization of (4) for triangular mesh generation requires the determination of coordinate transformations $\tilde{x}(x,y)$, $\tilde{y}(x,y)$ to satisfy

$$(dx,dy)H(dx,dy)^t = (d\tilde{x})^2 + \epsilon(d\tilde{y})^2 \tag{5}$$

where H is the hessian matrix, and ϵ is the sign of $\det(H)$. We can see that the mesh density function $\sqrt{|f''(x)|}$ applied in one dimensional equidistribution is generalized to use the hessian matrix. The constant ϵ appears in the canonical form (5) since the hessian matrix is not positive (nor negative) definite for a saddle shape function. Note that by the same strategy of transforming a uniform mesh into an optimal mesh, we see that the error equilibrating property of optimal meshes in one dimension is extended to two dimensions.

The conditions for finding transformations $\tilde{x}(x,y)$, $\tilde{y}(x,y)$ are in a classical result in differential geometry on the characterization of a "flat" space. To be consistent with notation used in differential geometry, we rename the original space coordinates (x,y) to (x_1,x_2), the transformed coordinates $(\tilde{x},\tilde{y})$ to (y_1,y_2) and entries in the hessian matrix as $\{g_{ij}\}$. Let $y_1(x_1,x_2)$, $y_2(x_1,x_2)$ be the required transformation, then

$$\begin{aligned}
(dy_1)^2 + \epsilon(dy_2)^2 &= \left(\frac{\partial y_1}{\partial x_1}dx_1 + \frac{\partial y_1}{\partial x_2}dx_2\right)^2 + \epsilon\left(\frac{\partial y_2}{\partial x_1}dx_1 + \frac{\partial y_2}{\partial x_2}dx_2\right)^2 \\
&= \left(\left(\frac{\partial y_1}{\partial x_1}\right)^2 + \epsilon\left(\frac{\partial y_2}{\partial x_1}\right)^2\right)(dx_1)^2 + \left(\left(\frac{\partial y_1}{\partial x_2}\right)^2 + \epsilon\left(\frac{\partial y_2}{\partial x_2}\right)^2\right)(dx_2)^2 \\
&\qquad +2\left(\frac{\partial y_1}{\partial x_1}\frac{\partial y_1}{\partial x_2} + \epsilon\frac{\partial y_2}{\partial x_1}\frac{\partial y_2}{\partial x_2}\right)dx_1dx_2 \\
&= g_{11}(dx_1)^2 + 2g_{12}(dx_1)(dx_2) + g_{22}(dx_2)^2
\end{aligned} \tag{6}$$

Therefore the transformation being sought must satisfy

$$
\begin{aligned}
g_{11} &= \left(\frac{\partial y_1}{\partial x_1}\right)^2 + \epsilon\left(\frac{\partial y_2}{\partial x_1}\right)^2 \\
g_{12} &= \frac{\partial y_1}{\partial x_1}\frac{\partial y_1}{\partial x_2} + \epsilon\frac{\partial y_2}{\partial x_1}\frac{\partial y_2}{\partial x_2} \\
g_{22} &= \left(\frac{\partial y_1}{\partial x_2}\right)^2 + \epsilon\left(\frac{\partial y_2}{\partial x_2}\right)^2
\end{aligned} \tag{7}
$$

3.2. A Classical Result in Differential Geometry. The basic question in differential geometry is, given a symmetric tensor $g_{ij}(x)$, under what restrictions on g_{ij} can there be a coordinate system defined by

$$y_i = y_i(x_1, ..., x_n), \quad (i = 1, ..., n)$$

in which the transformed tensor $g_{ij}(x)$ has constant components h_{ij} everywhere. A classical result in differential geometry gives the necessary and sufficient conditions on $g_{ij}(x)$. Details can be found in text books such as [16,17].

THEOREM 1. *[16, page 96] A necessary and sufficient condition that a symmetric tensor $g_{ij}(x)$, with $|g_{ij}| \neq 0$, reduce under a suitable transformation of coordinates to a tensor h_{ij}, where the h_{ij}'s are constants, is that the Riemann-Christoffel tensor formed from the g_{ij}'s be a zero tensor.*

Synge and Schild in their book [17] have shown that the quadratic form

$$(ds)^2 = h_{11}dy_1{}^2 + h_{22}dy_2{}^2 + 2h_{12}dy_1dy_2 \tag{8}$$

can be further reduced by a non-singular linear transformation to

$$(ds)^2 = d\tilde{y}_1{}^2 + \epsilon d\tilde{y}_2{}^2 \tag{9}$$

where ϵ is sign of $\det(h_{ij})$.

For the special case where the metric matrix $\{g_{ij}\}$ is a hessian matrix, the Christoffel symbols simplify to the following:
To simplify notation, let

$$
\begin{aligned}
g_{111} &= \frac{\partial g_{11}}{\partial x_1}, \quad g_{112} = \frac{\partial g_{11}}{\partial x_2} = \frac{\partial g_{12}}{\partial x_1} \\
g_{222} &= \frac{\partial g_{22}}{\partial x_2}, \quad g_{122} = \frac{\partial g_{12}}{\partial x_2} = \frac{\partial g_{22}}{\partial x_1} \\
g &= g_{11}g_{22} - g_{12}{}^2
\end{aligned}
$$

Then the Christoffel symbols of the second kind are,

$$\left\{ \begin{matrix} 1 \\ 11 \end{matrix} \right\} = \frac{g_{22}g_{111} - g_{12}g_{112}}{2g}, \quad \left\{ \begin{matrix} 2 \\ 11 \end{matrix} \right\} = \frac{g_{11}g_{112} - g_{12}g_{111}}{2g}$$

$$\left\{ \begin{matrix} 1 \\ 12 \end{matrix} \right\} = \frac{g_{22}g_{112} - g_{12}g_{122}}{2g} \quad , \quad \left\{ \begin{matrix} 1 \\ 22 \end{matrix} \right\} = \frac{g_{22}g_{122} - g_{12}g_{222}}{2g}$$
$$\left\{ \begin{matrix} 2 \\ 22 \end{matrix} \right\} = \frac{g_{11}g_{222} - g_{12}g_{122}}{2g} \quad , \quad \left\{ \begin{matrix} 2 \\ 12 \end{matrix} \right\} = \frac{g_{11}g_{122} - g_{12}g_{112}}{2g}$$

and the independent components of the Riemann-Christoffel symbols can be simplified to,

$$\begin{aligned} R^1_{212} &= \frac{g_{22}}{4g^2}\Gamma \quad , \quad R^1_{112} = \frac{g_{12}}{4g^2}\Gamma \\ R^2_{212} &= \frac{-g_{12}}{4g^2}\Gamma \quad , \quad R^2_{112} = \frac{-g_{11}}{4g^2}\Gamma \\ \Gamma &= g_{11}({g_{122}}^2 - g_{222}g_{112}) + g_{12}(g_{111}g_{222} - g_{112}g_{122}) + \\ &\qquad g_{22}({g_{112}}^2 - g_{122}g_{111}) \end{aligned} \tag{10}$$

One can easily verify that if for some constants K_1, K_2, K_3, the entries in the metric matrix satisfy,

$$K_1 g_{11} + K_2 g_{12} + K_3 g_{22} = 0$$

then the Riemann-Christoffel tensor given by (10) vanish identically. In particular, harmonic and quadratic functions satisfy the above condition.

Sokolnikoff [16, page 93] shows that $y_1(x_1, x_2)$, $y_2(x_1, x_2)$ satisfy the same system of first-order partial differential equations

$$\begin{aligned} \frac{\partial y_1}{\partial x_1} &= u_1 \\ \frac{\partial y_1}{\partial x_2} &= u_2 \end{aligned}$$

(11)

$$\begin{aligned} \frac{\partial u_1}{\partial x_1} &= \left\{ \begin{matrix} 1 \\ 11 \end{matrix} \right\} u_1 + \left\{ \begin{matrix} 2 \\ 11 \end{matrix} \right\} u_2 \\ \frac{\partial u_2}{\partial x_2} &= \left\{ \begin{matrix} 1 \\ 22 \end{matrix} \right\} u_1 + \left\{ \begin{matrix} 2 \\ 22 \end{matrix} \right\} u_2 \end{aligned}$$

3.3. Initial Value Problem. Due to the special structure of the exact differential equation in (11), $y_1(x_1, x_2)$ can be integrated as the solution to an initial value problem.

From (11) and by a basic property of line integrals,

$$\begin{aligned} y_1(x_1, x_2) - y_1(a, b) &= \int_P^Q dy_1 \\ &= \int_P^Q \frac{\partial y_1}{\partial x_1} dx_1 + \frac{\partial y_1}{\partial x_2} dx_2 \\ &= \int_P^Q u_1 dx_1 + u_2 dx_2 \end{aligned}$$

where the line integral from $P : (a,b)$ to $Q : (x_1,x_2)$ is path independent. Let $(x_1(t),x_2(t))$ be a parametrization of a continuous curve from (a,b) to (x_1,x_2). Then (11) can be formulated as a system of ordinary differential equations,

$$
\begin{aligned}
x'_1 &= \frac{d}{dt}x_1(t) \quad , \quad x'_2 = \frac{d}{dt}x_2(t) \\
\frac{d}{dt}y_1 &= u_1x'_1 + u_2x'_2 \\
\frac{d}{dt}u_1 &= \left(\left\{ \begin{array}{c} 1 \\ 11 \end{array} \right\} x'_1 + \left\{ \begin{array}{c} 1 \\ 12 \end{array} \right\} x'_2\right) u_1 + \left(\left\{ \begin{array}{c} 2 \\ 11 \end{array} \right\} x'_1 + \left\{ \begin{array}{c} 2 \\ 12 \end{array} \right\} x'_2\right) u_2 \\
\frac{d}{dt}u_2 &= \left(\left\{ \begin{array}{c} 1 \\ 12 \end{array} \right\} x'_1 + \left\{ \begin{array}{c} 1 \\ 22 \end{array} \right\} x'_2\right) u_1 + \left(\left\{ \begin{array}{c} 2 \\ 12 \end{array} \right\} x'_1 + \left\{ \begin{array}{c} 2 \\ 22 \end{array} \right\} x'_2\right) u_2
\end{aligned}
\tag{12}
$$

If the function to be approximated is a harmonic function, (12) can be further simplified to

$$
\begin{aligned}
\frac{d}{dt}y_1 &= u_1x'_1 + u_2x'_2 \\
\frac{d}{dt}u_1 &= (\alpha x'_1 + \beta x'_2)u_1 - (\beta x'_1 - \alpha x'_2)u_2 \\
\frac{d}{dt}u_2 &= (\beta x'_1 - \alpha x'_2)u_1 + (\alpha x'_1 + \beta x'_2)u_2 \\
\alpha &= \frac{1}{4}\frac{\partial}{\partial x_1}\ln|\det(H)| \quad , \quad \beta = \frac{1}{4}\frac{\partial}{\partial x_2}\ln|\det(H)|
\end{aligned}
\tag{13}
$$

Hence with initial conditions for $y_1(a,b)$, $u_1(a,b)$, $u_2(a,b)$, (12) can be solved as an initial value problem. In particular, the path of integration can be chosen to be taken along only horizontal and vertical directions. First integrate horizontally from (a,b) to (x_1,b) by

$$
\begin{aligned}
x_1(t) &= t \quad , \quad x'_1(t) = 1 \quad , \quad a \le t \le x_1 \\
x_2(t) &= b \quad , \quad x'_2(t) = 0
\end{aligned}
\tag{14}
$$

then vertically from (x_1,b) to (x_1,x_2) by

$$
\begin{aligned}
x_1(t) &= x_1 \quad , \quad x'_1(t) = 0 \\
x_2(t) &= t \quad , \quad x'_2(t) = 1 \quad , \quad b \le t \le x_2
\end{aligned}
\tag{15}
$$

Since $y_2(x_1,x_2)$ also satisfies (11) and therefore (12), $y_2(x_1,x_2)$ can similarly be integrated as $y_1(x_1,x_2)$. The coefficients in the transformed metric tensor are constants and obviously independent of (y_1,y_2), therefore the tensor can be determined

by consideration at any point. To achieve (9) and to be consistent with transformation used in local quadratic model, the initial values of (u_1, u_2), for $y_1(x_1, x_2)$, $y_2(x_1, x_2)$, are chosen to be the orthogonal scaled eigenvectors of the hessian matrix at (a, b),

$$(u_1, u_2) = \sqrt{|\lambda_1|}(q_{11}, q_{21}) \tag{16}$$

for $y_1(x_1, x_2)$ and for $y_2(x_1, x_2)$,

$$(u_1, u_2) = \sqrt{|\lambda_2|}(q_{12}, q_{22}) \tag{17}$$

where

$$Q = \begin{pmatrix} q_{11} & q_{12} \\ q_{21} & q_{22} \end{pmatrix} \quad , \quad Q^t H Q = \begin{pmatrix} \lambda_1 & 0 \\ 0 & \lambda_2 \end{pmatrix}$$

The metric tensor then satisfies (9). Therefore, the coordinate transformation $y_1(x_1, x_2)$, $y_2(x_1, x_2)$ can be numerically computed as solutions to initial value problems.

3.4. Conformal Mapping. If the function to be approximated is a harmonic function, the coordinate transformations, $(y_1(x_1, x_2), y_2(x_1, x_2))$ determined by initial conditions (16), (17) can be shown to be a conformal mapping. Now the transformed metric tensor is diagonal, hence the gradient vectors for $y_1(x_1, x_2)$, $y_2(x_1, x_2)$ are orthogonal,

$$\frac{\partial y_1}{\partial x_1}\frac{\partial y_2}{\partial x_1} + \frac{\partial y_1}{\partial x_2}\frac{\partial y_2}{\partial x_2} = 0 \tag{18}$$

By (7) the transformations $(y_1(x_1, x_2), y_2(x_1, x_2))$ satisfy

$$\begin{aligned} g_{11} &= \left(\frac{\partial y_1}{\partial x_1}\right)^2 - \left(\frac{\partial y_2}{\partial x_1}\right)^2 \\ g_{22} &= -g_{11} = \left(\frac{\partial y_1}{\partial x_2}\right)^2 - \left(\frac{\partial y_2}{\partial x_2}\right)^2 \end{aligned}$$

which implies

$$\frac{\partial y_1}{\partial x_1}^2 + \frac{\partial y_1}{\partial x_2}^2 = \frac{\partial y_2}{\partial x_1}^2 + \frac{\partial y_2}{\partial x_2}^2 \tag{19}$$

From (18) and (19), we can show either,

$$\frac{\partial y_1}{\partial x_1} = \frac{\partial y_2}{\partial x_2} \quad , \quad \frac{\partial y_1}{\partial x_2} = -\frac{\partial y_2}{\partial x_1} \tag{20}$$

or

$$\frac{\partial y_1}{\partial x_2} = \frac{\partial y_2}{\partial x_1} \quad , \quad \frac{\partial y_1}{\partial x_1} = -\frac{\partial y_2}{\partial x_2} \tag{21}$$

We recognize (20) and (21) are related by exchange of coordinates x_1, x_2 and (20) as the Cauchy-Riemann equations for a complex function. Therefore $(y_1(x_1, x_2), y_2(x_1, x_2))$ is a conformal mapping. Note in contrast to the classical applications of conformal mappings, this mapping is determined by consideration of error properties and *not* by geometric considerations of transforming the region of computation to some canonical domain.

4. Numerical Experiments. In this section, we shall examine some results from numerical experiments of optimal mesh generation for interpolating a harmonic function over the unit square. Three mesh generation strategies are used for each example. One strategy is to generate a mesh by mapping a regular mesh of optimal shape triangles into the *interior* of the unit square. To cover the unit square exactly, boundary triangles must be distorted from the optimal shape to fit the boundary edges, thus incurring a change in error properties. This phenomenon is exhibited by a mesh obtained by tiling the transformed unit square with equilateral triangles. The equilateral triangles are generated by **D03MAF** of the **NAG** library. Lastly, we included a mesh obtained by **PLTMG**. **PLTMG**[1] is a multigrid package with adaptive triangular mesh refinement for solving second order partial differential equations. Since a triangular mesh in **PLTMG** is stored in a complicated data structure of nested trees of triangles, the mesh node positions from **PLTMG** are simply extracted to form a delaunay triangulation to be used in this comparison. The maximum interpolation error over each triangle is plotted in ascending order to form an error profile. Ideally, by the equilibrating property of an optimal mesh, the error profile should be almost level.

D02CBF, a variable step Adams code in the **NAG** library, integrates the initial value problem (12) as described in (14) and (15), to yield values of $y_1(x_1, x_2)$, $y_2(x_1, x_2)$ over a regular 40×40 grid. Note that the unit square is distorted over the transformed plane by the coordinate transformation. **D03MAF** of the **NAG** library triangulates this distorted region by equilateral triangles. The corresponding triangulation in the original coordinates is determined by the inverse mapping of this regular mesh. The inverse mapping is computed by assuming that each rectangular cell on the square grid determines a bilinear function. More sophisticated bicubic splines approximation and numerical techniques for inverse mapping had been tried and found to give no significant improvements over this simple technique.

The triangular meshes produced by **D03MAF** are compared against meshes generated by **PLTMG** , in solving Laplace's problem with Dirichlet boundary conditions. A regular triangulation by optimal shape triangles over the *interior* of the domain is used to demonstrate the equilibrating property and act as a indicator of closeness of **PLTMG** to an optimal mesh. The comparison is not precise since the number of triangles used cannot be tightly controlled.

Four interpolation examples are chosen to demonstrate the effectiveness of optimal mesh generation by coordinate transformation. Since these examples exhibit sharp increases, we expect to see triangles sizes to vary accordingly.

Example 1 Exponential increase along x_1-axis

$$f(x_1, x_2) = \exp(5x_1)\sin(5x_2)$$

The coordinate transformations are

$$y_1(x_1, x_2) = \frac{2}{\sqrt{2}}(\exp(5x_1/2)(\cos(5x_2/2) + \sin(5x_2/2)) - 1)$$

$$y_2(x_1,x_2) = \frac{2}{\sqrt{2}}(\exp(5x_1/2)(\cos(5x_2/2)-\sin(5x_2/2))-1)$$

Example 2 A near singularity with $z = x + Iy$ and $z_0 = x_0 + Iy_0 = (1/2) - (1/5)I$

$$\begin{aligned} f(x_1,x_2) &= \Re e\ 1/(z-z_0)^2 \\ &= \frac{(x_1-x_0)^2-(x_2-y_0)^2}{((x_1-x_0)^2+(x_2-y_0)^2)^2} \end{aligned}$$

The coordinate transformations are

$$\begin{aligned} y_1(x_1,x_2) &= \sqrt{6}\left(1-\frac{x_1-x_0}{(x_1-x_0)^2+(x_2-y_0)^2}\right) \\ y_2(x_1,x_2) &= \sqrt{6}\frac{x_2-y_0}{(x_1-x_0)^2+(x_2-y_0)^2} \end{aligned}$$

Example 3 A more severe near singularity

$$\begin{aligned} f(x_1,x_2) &= \Re e\ 1/(z-z_0)^4 \\ &= \frac{((x_1-x_0)^2+(x_2-y_0)^2)^2-8(x_1-x_0)^2(x_2-y_0)^2}{((x_1-x_0)^2+(x_2-y_0)^2)^4} \end{aligned}$$

The coordinate transformations are

$$\begin{aligned} y_1(x_1,x_2) &= \sqrt{5}\left(1+\frac{(x_2-y_0)^2-(x_1-x_0)^2}{((x_1-x_0)^2+(x_2-y_0)^2)^2}\right) \\ y_2(x_1,x_2) &= 2\sqrt{5}\frac{(x_1-x_0)(x_2-y_0)}{((x_1-x_0)^2+(x_2-y_0)^2)^2} \end{aligned}$$

Example 4 Example 2 is modified by a rescaling of x_2-variable to satisfy

$$\frac{\partial^2 f}{\partial x_1 \partial x_1} + 10\frac{\partial^2 f}{\partial x_2 \partial x_2} = 0$$

Then

$$f(x_1,x_2) = \frac{(x_1-x_0)^2-(\sqrt{5}x_2-y_0)^2}{((x_1-x_0)^2+(\sqrt{5}x_2-y_0)^2)^2}$$

The results of the numerical experiments are summarized in Tables 1, 2, 3 and 4. Error profiles for the four problems are contained in Figures 2, 3, 4, 5. Meshes obtained by transformation of optimal shape triangles show an almost level error profile and remarkable equilibrating properties in agreement with theoretical prediction (see Figures 10, 15, 20, 25). Meshes produced by **D03MAF** by tiling the transformed domain by equilateral triangles are shown in Figures 8, 13, 18 and 23. The error profile shows

TABLE 1
Summary of results for Example 1

$f(x_1, x_2) = \exp(5x_1)\sin(5x_2)$					
	minimum error	median error	90 percentile	maximum error	number of triangles
optimal	13.60d-2	13.79d-2	13.94d-2	14.16d-2	1098
shape	5.273d-2	5.390d-2	5.498d-2	5.740d-2	2933
equilateral	1.945d-2	6.644d-2	6.793d-2	14.88d-2	3190
PLTMG	1.912d-2	7.600d-2	14.10d-2	21.77d-2	3080

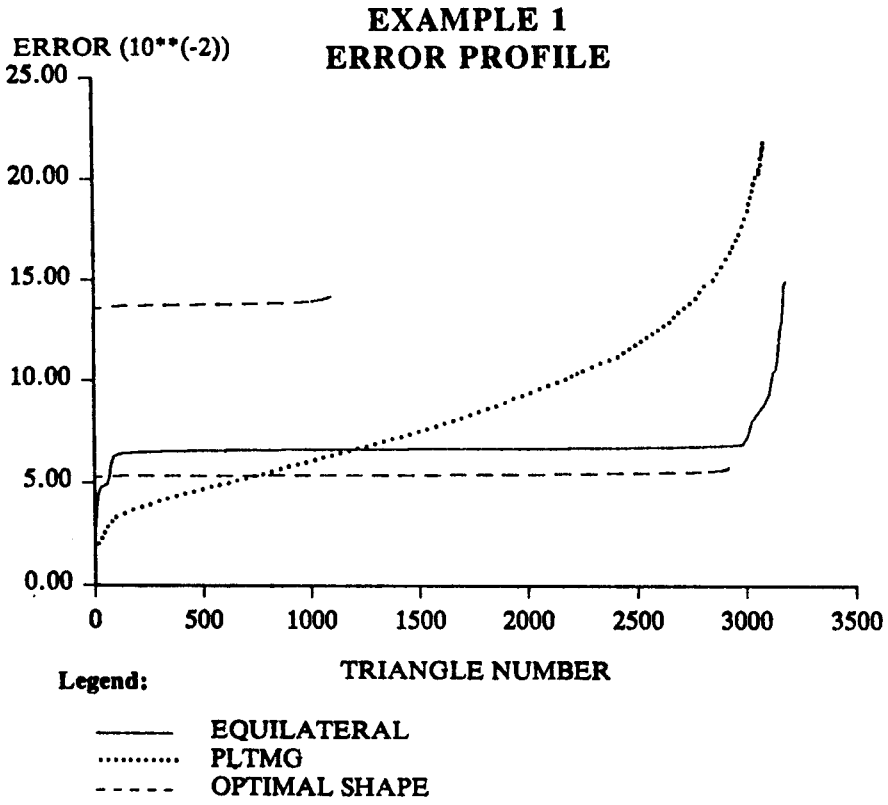

FIG. 2. *Error profiles for Example 1*

TABLE 2
Summary of results for Example 2

$f(x_1, x_2) = \Re e\ 1/(z - z_0)^2$					
	minimum error	median error	90 percentile	maximum error	number of triangles
optimal	4.442d-2	4.680d-2	4.853d-2	5.310d-2	436
shape	1.876d-2	2.009d-2	2.155d-2	2.566d-2	1072
equilateral	0.747d-2	2.181d-2	2.320d-2	4.616d-2	1376
PLTMG	0.848d-2	2.890d-2	5.213d-2	8.426d-2	1168

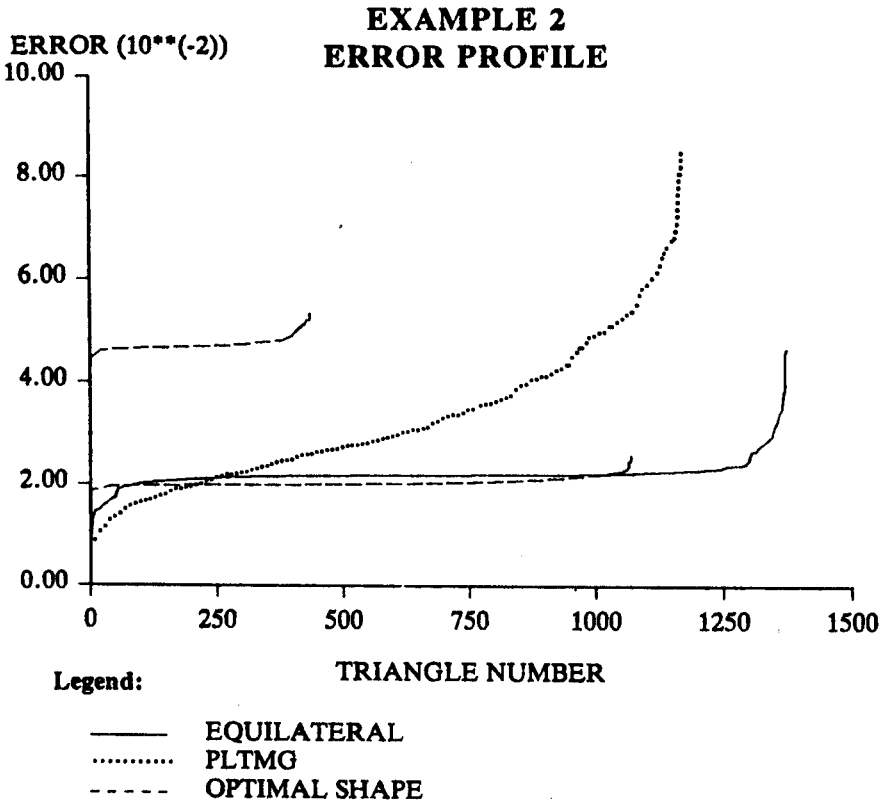

FIG. 3. *Error profiles for Example 2*

TABLE 3
Summary of results for Example 3

$f(x_1, x_2) = \Re e\ 1/(z - z_0)^4$					
	minimum error	median error	90 percentile	maximum error	number of triangles
optimal	2.146d-2	2.366d-2	2.597d-2	3.379d-2	300
shape	1.021d-2	1.160d-2	1.322d-2	1.696d-2	650
equilateral	0.837d-2	1.567d-2	1.886d-2	3.725d-2	661
PLTMG	0.145d-2	1.690d-2	3.055d-2	5.184d-2	720

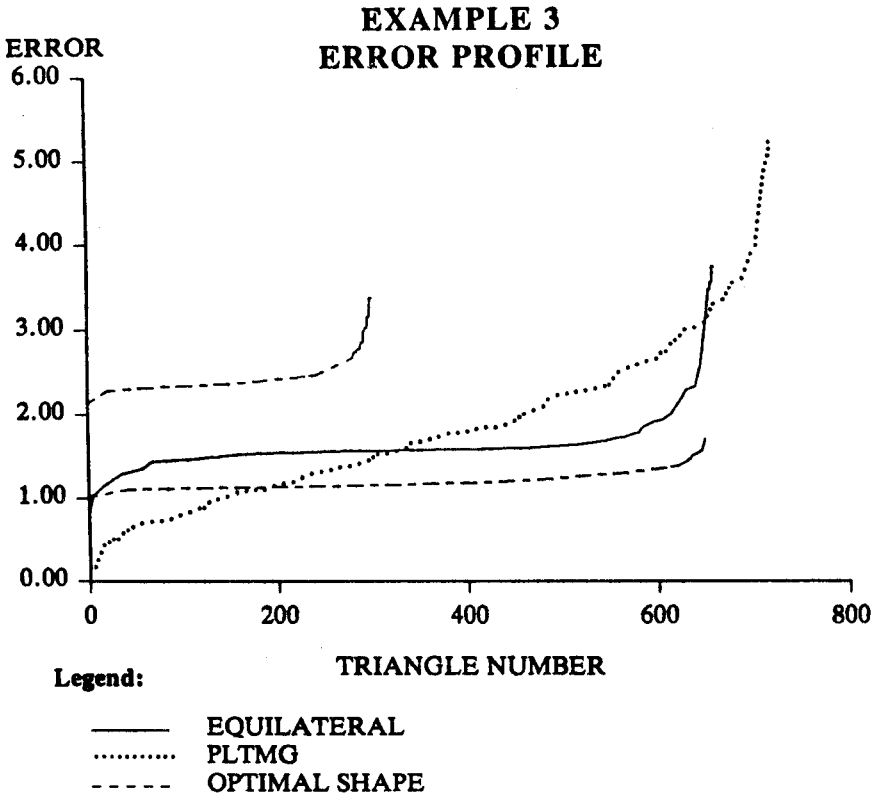

FIG. 4. *Error profiles for Example 3*

TABLE 4
Summary of results for Example 4

	minimum error	median error	90 percentile	maximum error	number of triangles
optimal	10.15d-2	12.46d-2	14.61d-2	18.10d-2	162
shape	2.433d-2	3.169d-2	4.059d-2	6.004d-2	711
equilateral	1.990d-2	4.237d-2	5.665d-2	11.35d-2	701
PLTMG	0.368d-2	5.914d-2	18.44d-2	47.23d-2	796

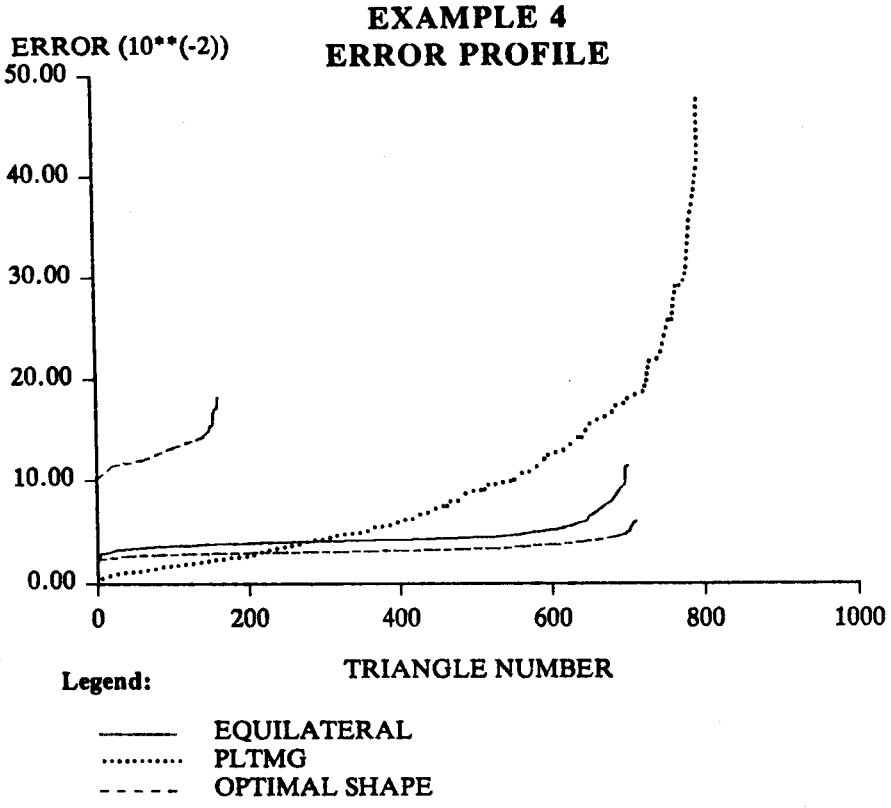

FIG. 5. *Error profiles for Example 4*

a level curve with an abrupt increase in error. The anomalous increases are caused by distortion of triangle geometry along the boundary (see Figures 11, 16, 21). Note that by the maximum principle, extremal values of harmonic functions occur also along the boundary. Figures 9, 14, 19, and 24, show the corresponding meshes produced by PLTMG.

Although PLTMG produces meshes without the equilibrating property and incur larger maximum errors, for the purpose of finite element computation, such meshes can be considered to be "near" optimal since their errors are within a small multiple of the theoretical optimum. In another perspective, the error tolerance for meshes produced by PLTMG can be similarly obtained by meshes produced through coordinate transformation with only a fraction of number of triangles.

5. Conclusion. This paper is a basic study on optimal meshes with the intention of providing insight into more complex optimal mesh problems in finite element computation. The motivation and development of coordinate transformation for generating optimally efficient meshes have been presented. The effectiveness of such a strategy is demonstrated by the numerical examples. We conclude that mesh generation by coordinate transformation is a promising strategy in the investigation of optimal meshes.

The existence of a global coordinate transformation for optimally efficient mesh generation relies on $f(x_1, x_2)$ satisfying (10). An interesting question is whether the class of functions in C^3 and satisfy (10) is dense in L_∞ norm. Note that harmonic functions are in C^3 but not dense, and piecewise quadratic functions are dense but not in C^3.

Appendix A. In this section, we derive the error expression $E(x, y)$ obtained in the interpolation of a quadratic function

$$f(x, y) = (x, y)H(x, y)^t + d_1 x + d_2 y + d_3$$

over a triangle with vertices at (x_1, y_1), (x_2, y_2), (x_3, y_3). Let the error function be represented by

$$E(x, y) = -(x, y)H(x, y)^t + b_1 x + b_2 y + b_3$$

By the interpolation condition

$$E(x_1, y_1) = E(x_2, y_2) = E(x_3, y_3) = 0$$

The unknows b_1, b_2, b_3 can easily be obtained by solving the system of linear equations

$$\begin{pmatrix} x_1 & y_1 & 1 \\ x_2 & y_2 & 1 \\ x_3 & y_3 & 1 \end{pmatrix} \begin{pmatrix} b_1 \\ b_2 \\ b_3 \end{pmatrix} = \begin{pmatrix} r_1 \\ r_2 \\ r_3 \end{pmatrix}$$

where $r_i = (x_i, y_i)H(x_i, y_i)^t$. This gives

$$\begin{aligned} b_1 &= \frac{r_1(y_2 - y_3) + r_2(y_3 - y_1) + r_3(y_1 - y_2)}{2A} \\ b_2 &= \frac{r_1(x_3 - x_2) + r_2(x_1 - x_3) + r_3(x_2 - x_1)}{2A} \\ b_3 &= \frac{r_1(x_2y_3 - x_3y_2) + r_2(x_3y_1 - x_1y_3) + r_3(x_1y_2 - x_2y_1)}{2A} \end{aligned}$$

with A being the area of triangle

$$A = \frac{1}{2}(x_1(y_2 - y_3) + x_2(y_3 - y_1) + x_3(y_1 - y_2))$$

Let (x_c, y_c) be the solution of the linear equations

$$\begin{pmatrix} b_1/2 \\ b_2/2 \end{pmatrix} = H \begin{pmatrix} x_c \\ y_c \end{pmatrix} \quad \text{then} \quad x_c = \frac{b_1h_{22} - h_{12}b_2}{2\det(H)} \quad , \quad y_c = \frac{b_2h_{11} - h_{12}b_1}{2\det(H)}$$

The error at displacement (dx, dy) from (x_c, y_c) is given by

$$\begin{aligned} E(x_c + dx, y_c + dy) &= -(x_c + dx, y_c + dy)H(x_c + dx, y_c + dy)^t + \\ &\qquad b_1(x_c + dx) + b_2(y_c + dy) + b_3 \\ &= -(x_c, y_c)H(x_c, y_c)^t - (dx, dy)H(dx, dy)^t \\ &\qquad -2(dx, dy)H(x_c, y_c)^t + b_1(x_c + dx) + b_2(y_c + dy) + b_3 \\ &= E(x_c, y_c) - (dx, dy)H(dx, dy)^t \end{aligned}$$

Finally, the expression $E(x_c, y_c)$ can be further simplified to

$$E(x_c, y_c) = \frac{D_{12}D_{23}D_{31}}{16A^2\det(H)}$$

where

$$\begin{aligned} D_{ij} &= (x_i - x_j, y_i - y_j)H(x_i - x_j, y_i - y_j)^t \\ &= h_{11}(x_i - x_j)^2 + 2(x_i - x_j)(y_i - y_j)h_{12} + h_{22}(y_i - y_j)^2 \end{aligned}$$

Appendix B. In this section, we shall find the geometry of an optimally efficient triangle for approximation of a saddle shape function. We recall from Section 2 that for a triangle over the transformed plane with vertices at $(\tilde{x}_1, \tilde{y}_1)$, $(\tilde{x}_2, \tilde{y}_2)$, $(\tilde{x}_3, \tilde{y}_3)$, the local maximum error along edge $(\tilde{x}_i, \tilde{y}_i)$, $(\tilde{x}_j, \tilde{y}_j)$ is

$$E_{ij} = \frac{1}{4}|(\tilde{x}_i - \tilde{x}_j)^2 - (\tilde{y}_i - \tilde{y}_j)^2|$$

The triangle geometry shown in Figure 1 attains the same error on all three sides,

$$E_{12} = E_{23} = E_{31} \tag{22}$$

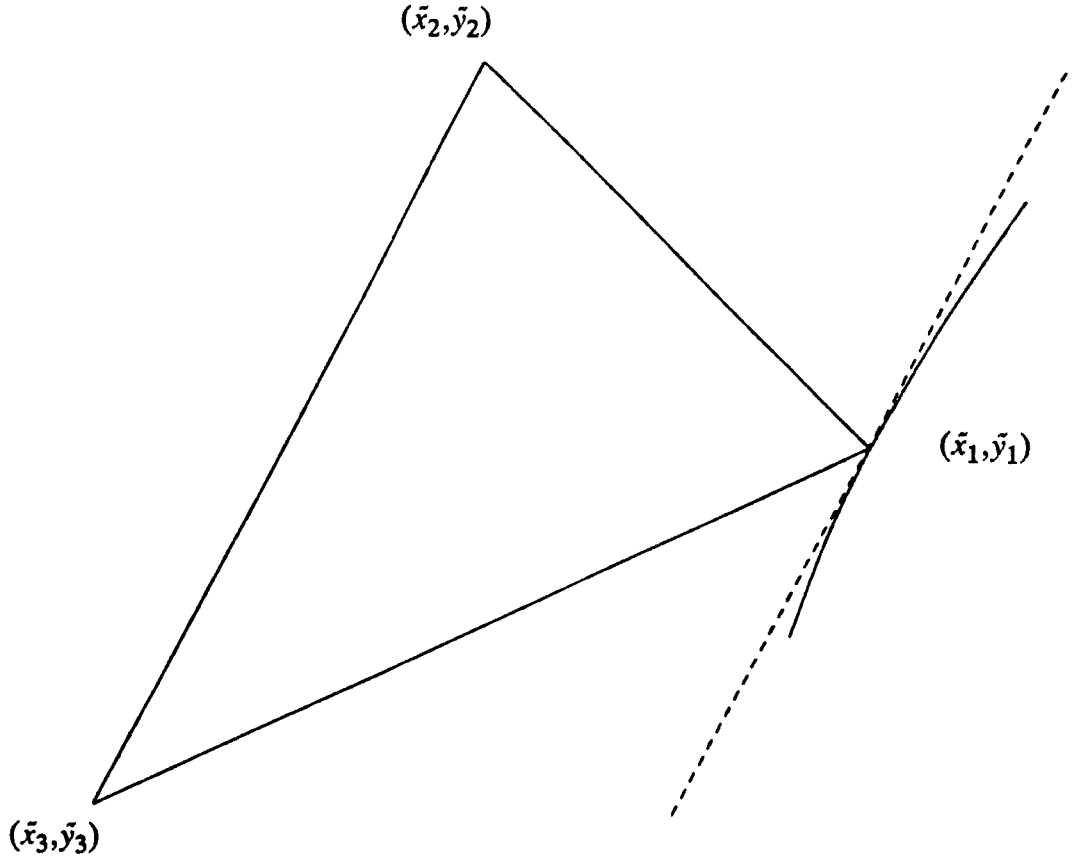

FIG. 6. $(\tilde{x}_1, \tilde{y}_1)$ *perturbed along the hyperbola*

We can show show that this equality of error on all sides is a necessary condition for an optimally efficient triangle. Assume the contrary that the error on one edge is strictly smaller,

$$E_{12} < E_{23} \quad , \quad E_{12} < E_{31}$$

Then $(\tilde{x}_1, \tilde{y}_1)$ can be perturbed along the hyperbola given by

$$(x - \tilde{x}_3)^2 - (y - \tilde{y}_3)^2 = (\tilde{x}_1 - \tilde{x}_3)^2 - (\tilde{y}_1 - \tilde{y}_3)^2$$

with no changes to E_{23} nor E_{31} (see Figure 6), however we note that the area of this triangle increases as $(\tilde{x}_1, \tilde{y}_1)$ is perturbed. The maximum error is unchanged but the area can be increased by such a perturbation, thus it cannot be optimally efficient.

Let us consider the problem of finding a triangle geometry which minimizes the squared ratio of Error to Area. and subject to condition (22) that all edges attain the same error. Let a triangle of arbitrary shape be described as having vertices at $(0,0)$, $(\cos\theta, \sin\theta)$, (x,y). Then the above conditions can be formulated as

$$\min \left(\frac{\text{Error}}{\text{Area}}\right)^2 = \min \frac{(\cos^2\theta - \sin^2\theta)^2}{4(y\cos\theta - x\sin\theta)^2} \tag{23}$$

subject to

$$x^2 - y^2 = \epsilon_1(\cos^2\theta - \sin^2\theta) \quad , \quad |\epsilon_1| = 1 \tag{24}$$

$$(x - \cos\theta)^2 - (y - \sin\theta)^2 = \epsilon_2(\cos^2\theta - \sin^2\theta) \quad , \quad |\epsilon_2| = 1 \tag{25}$$

Now from (25)

$$\begin{aligned} \epsilon_2(\cos^2\theta - \sin^2\theta) &= (x^2 - 2x\cos\theta + \cos^2\theta) - (y^2 - 2y\sin\theta + \sin^2\theta) \\ &= (x^2 - y^2) + (\cos^2\theta - \sin^2\theta) - 2(x\cos\theta - y\sin\theta) \end{aligned}$$

Hence equation (25) can be simplified to

$$2(x\cos\theta - y\sin\theta) = (\cos^2\theta - \sin^2\theta)(1 + \epsilon_1 - \epsilon_2) \tag{26}$$

Solving (26) and (24) yields two solutions for (x,y) given as

$$\begin{aligned} (x,y) &= (K/2\cos\theta - \sqrt{R}/2\sin\theta, K/2\sin\theta - \sqrt{R}/2\cos\theta) \\ (x,y) &= (K/2\cos\theta + \sqrt{R}/2\sin\theta, K/2\sin\theta + \sqrt{R}/2\cos\theta) \end{aligned}$$

where

$$K = (1 + \epsilon_1 - \epsilon_2) \quad , \quad R = 1 - 2(\epsilon_1 + \epsilon_2) + (\epsilon_1 - \epsilon_2)^2$$

For both values of (x,y), formula (23) reduces to

$$\frac{(\cos^2\theta - \sin^2\theta)^2}{4(y\cos\theta - x\sin\theta)^2} = \frac{16}{1 - 2(\epsilon_1 + \epsilon_2) + (\epsilon_1 - \epsilon_2)^2} = \frac{16}{R}$$

Expression R equals 5 except for $(\epsilon_1, \epsilon_2) = (1,1)$ where R is -3 which is impossible.

Thus for each orientation of angle θ, there are six configurations for an optimal shape triangle. The results are summarized in Table 5. In particular, for zero rotation ($\theta = 0$), the triangle shapes are displayed in Figure 7. Note the triangle geometry show in Figure 1 corresponds to triangle with vertex V_2.

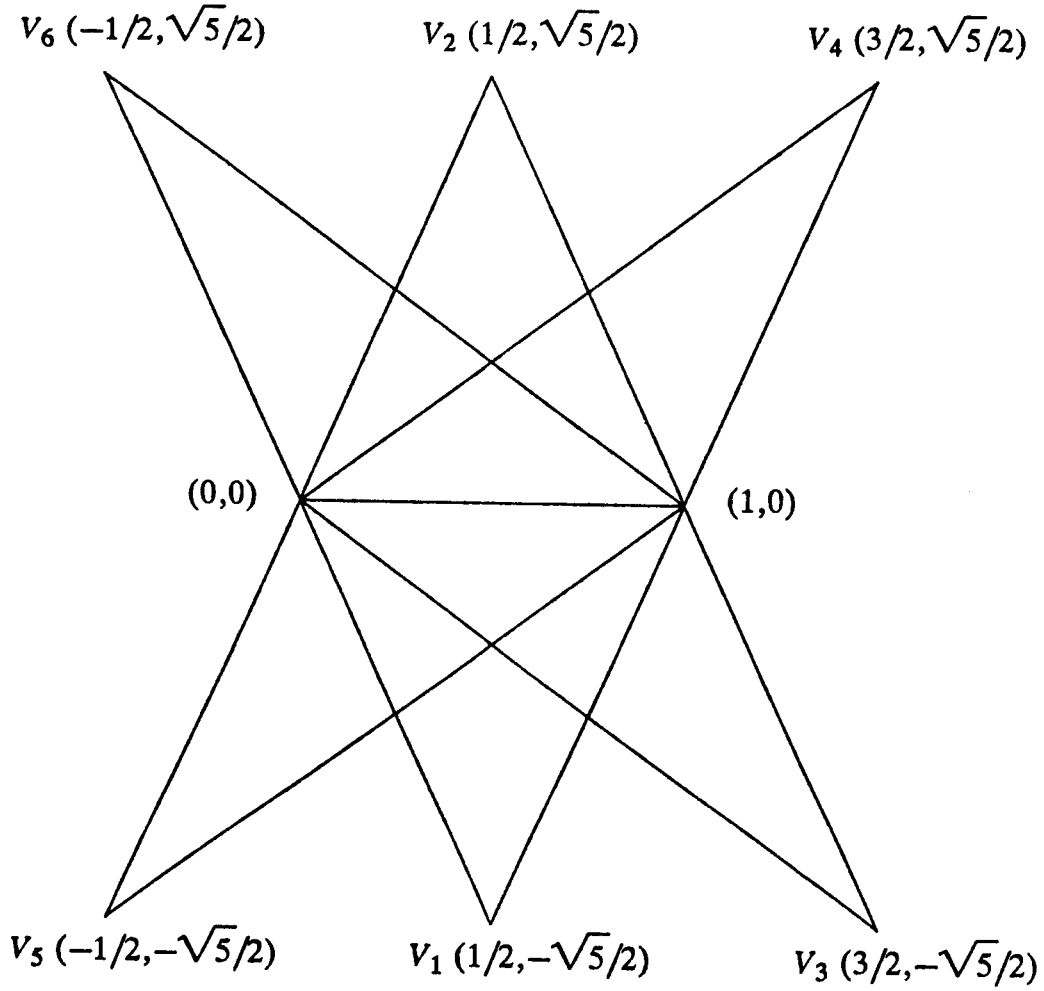

FIG. 7. *Optimal shape triangles for* $\theta = 0$

TABLE 5
Summary of results for (x, y)

$\epsilon_1 = -1$	$V_1 : (\sqrt{5}/2 \sin\theta + (1/2)\cos\theta, -\sqrt{5}/2 \cos\theta/2 + (1/2)\sin\theta)$
$\epsilon_2 = -1$	$V_2 : (\sqrt{5}/2 \sin\theta + (1/2)\cos\theta, \sqrt{5}/2 \cos\theta + (1/2)\sin\theta)$
$\epsilon_1 = 1$	$V_3 : (-\sqrt{5}/2 \sin\theta + 3/2 \cos\theta, 3/2 \sin\theta - \sqrt{5}/2 \cos\theta)$
$\epsilon_2 = -1$	$V_4 : (\sqrt{5}/2 \sin\theta + 3/2 \cos\theta, 3/2 \sin\theta + \sqrt{5}/2 \cos\theta)$
$\epsilon_1 = -1$	$V_5 : (-\sqrt{5}/2 \sin\theta - (1/2)\cos\theta, -(1/2)\sin\theta - \sqrt{5}/2 \cos\theta)$
$\epsilon_2 = 1$	$V_6 : (\sqrt{5}/2 \sin\theta - (1/2)\cos\theta, -(1/2)\sin\theta + \sqrt{5}/2 \cos\theta)$

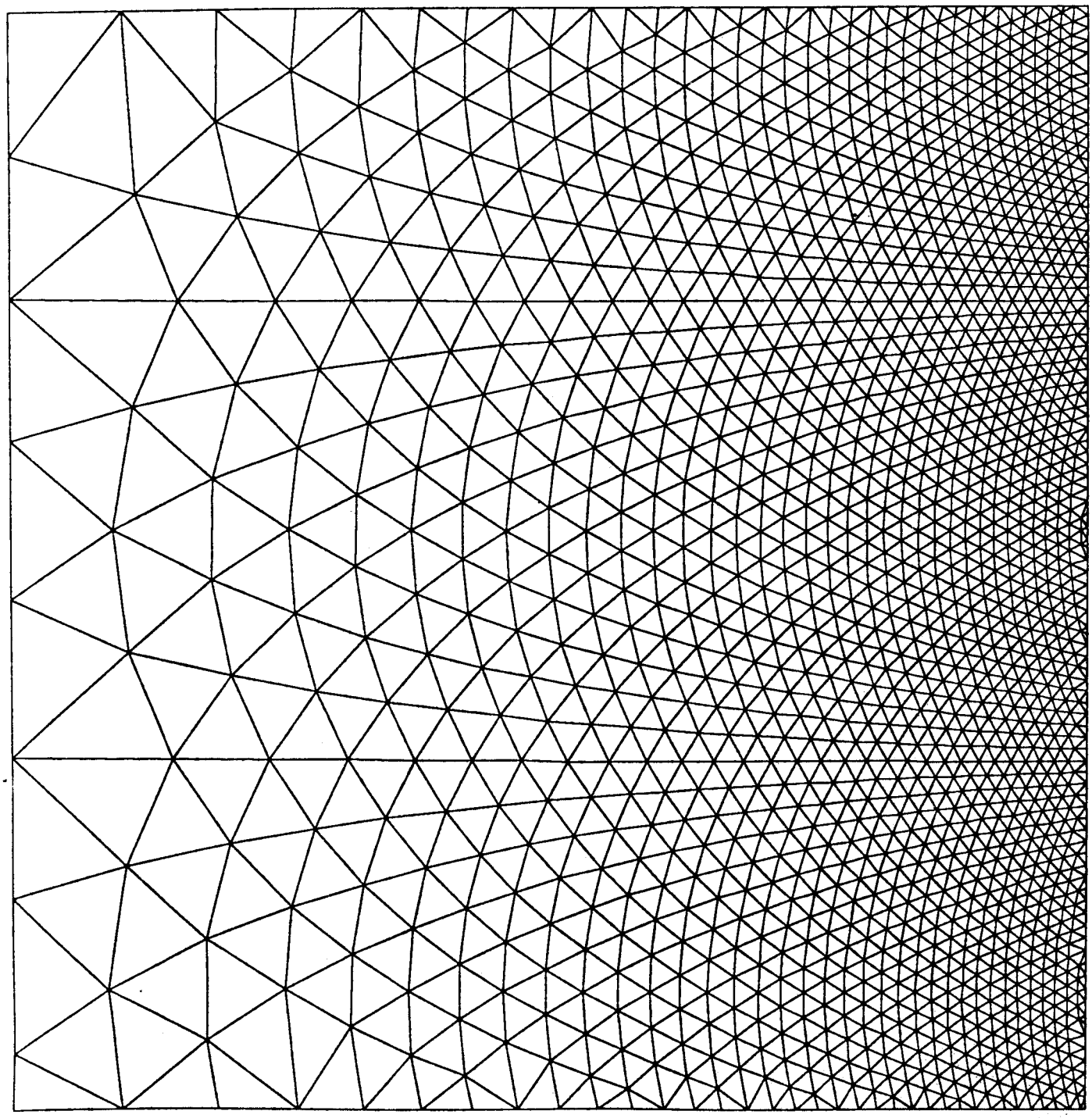

FIG. 8. *Mesh produced by equilateral triangles for Example 1*

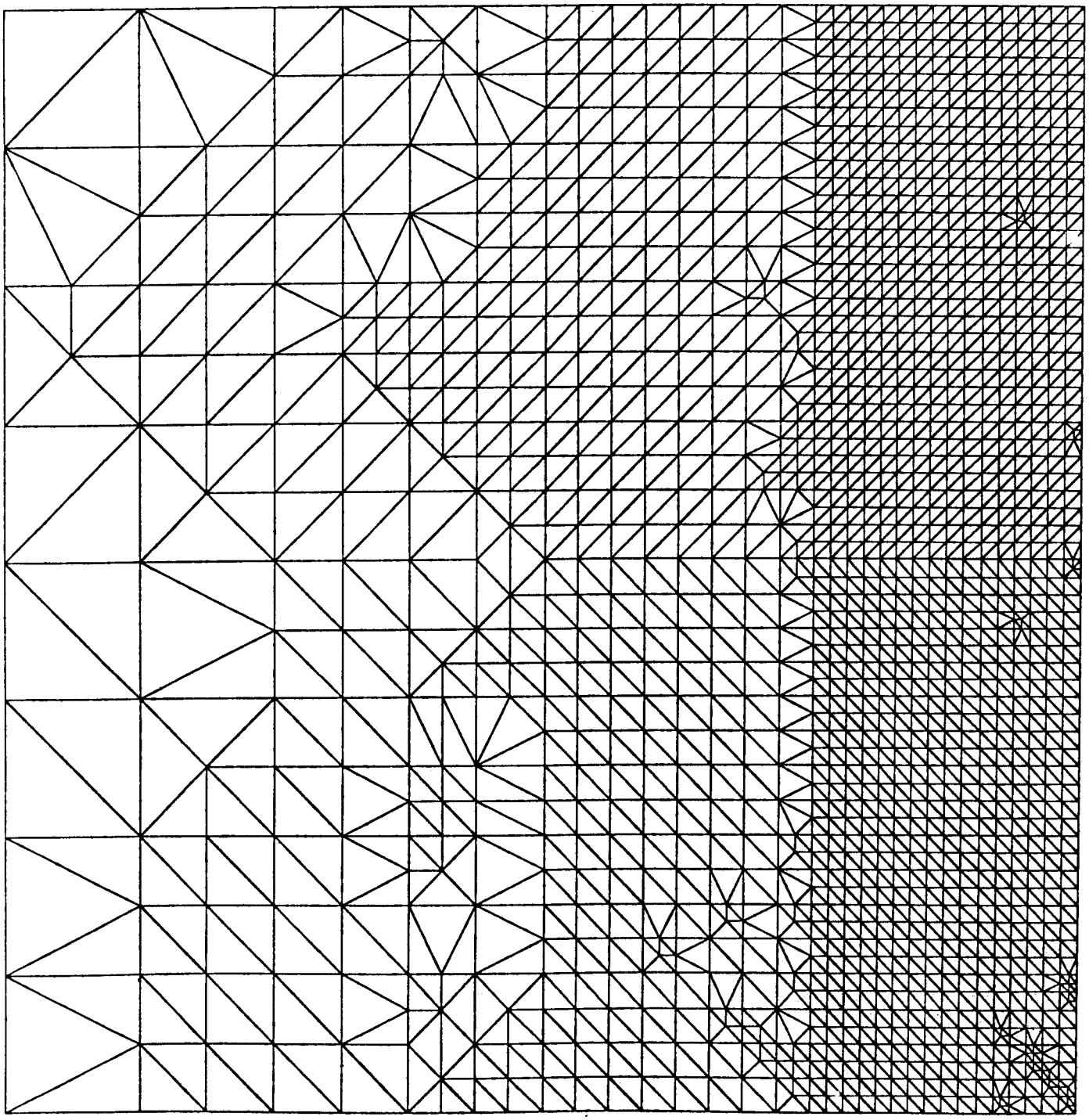

FIG. 9. *Mesh produced by* PLTMG *for Example 1*

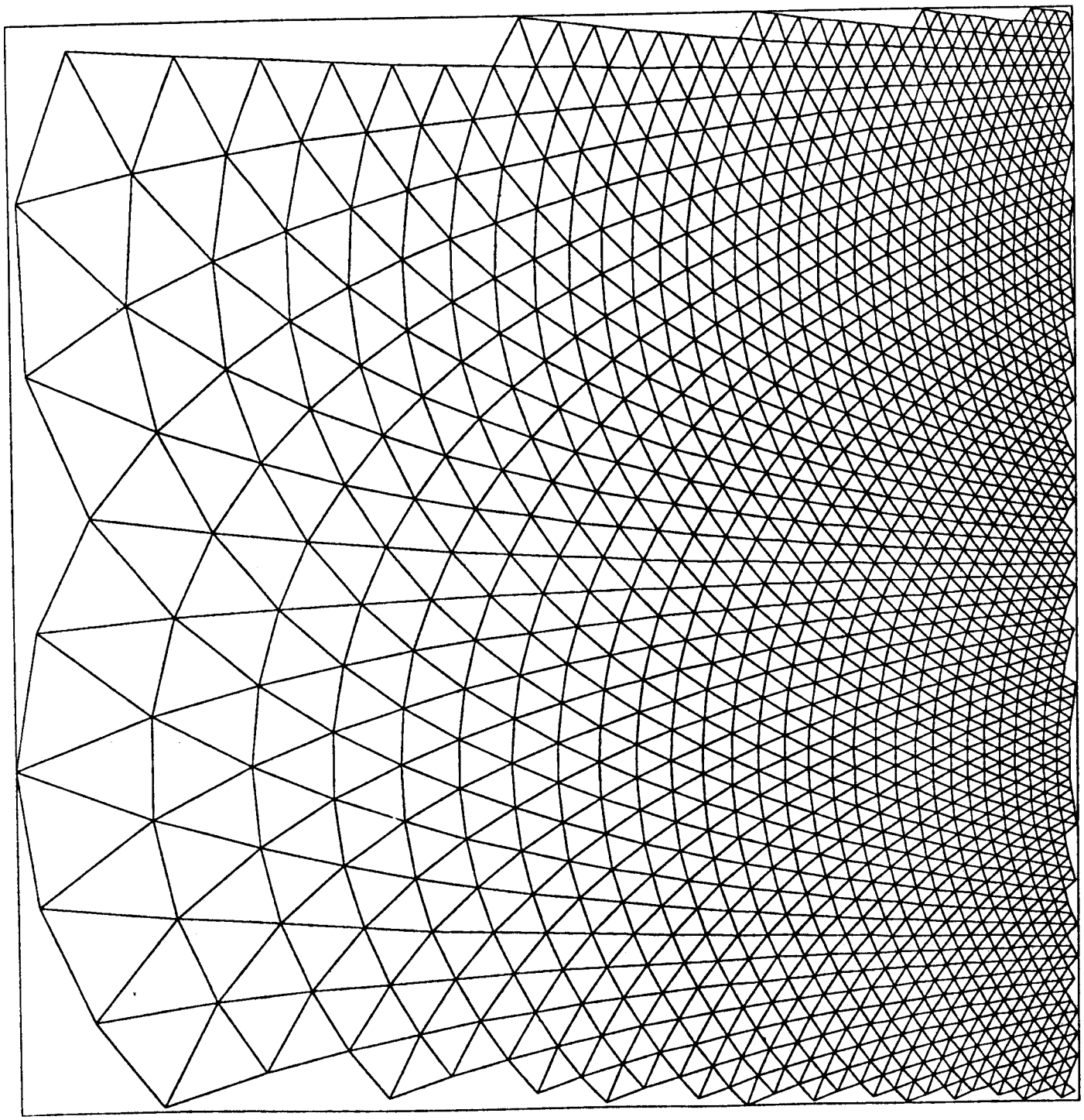

FIG. 10. *Optimally efficient triangulation for Example 1*

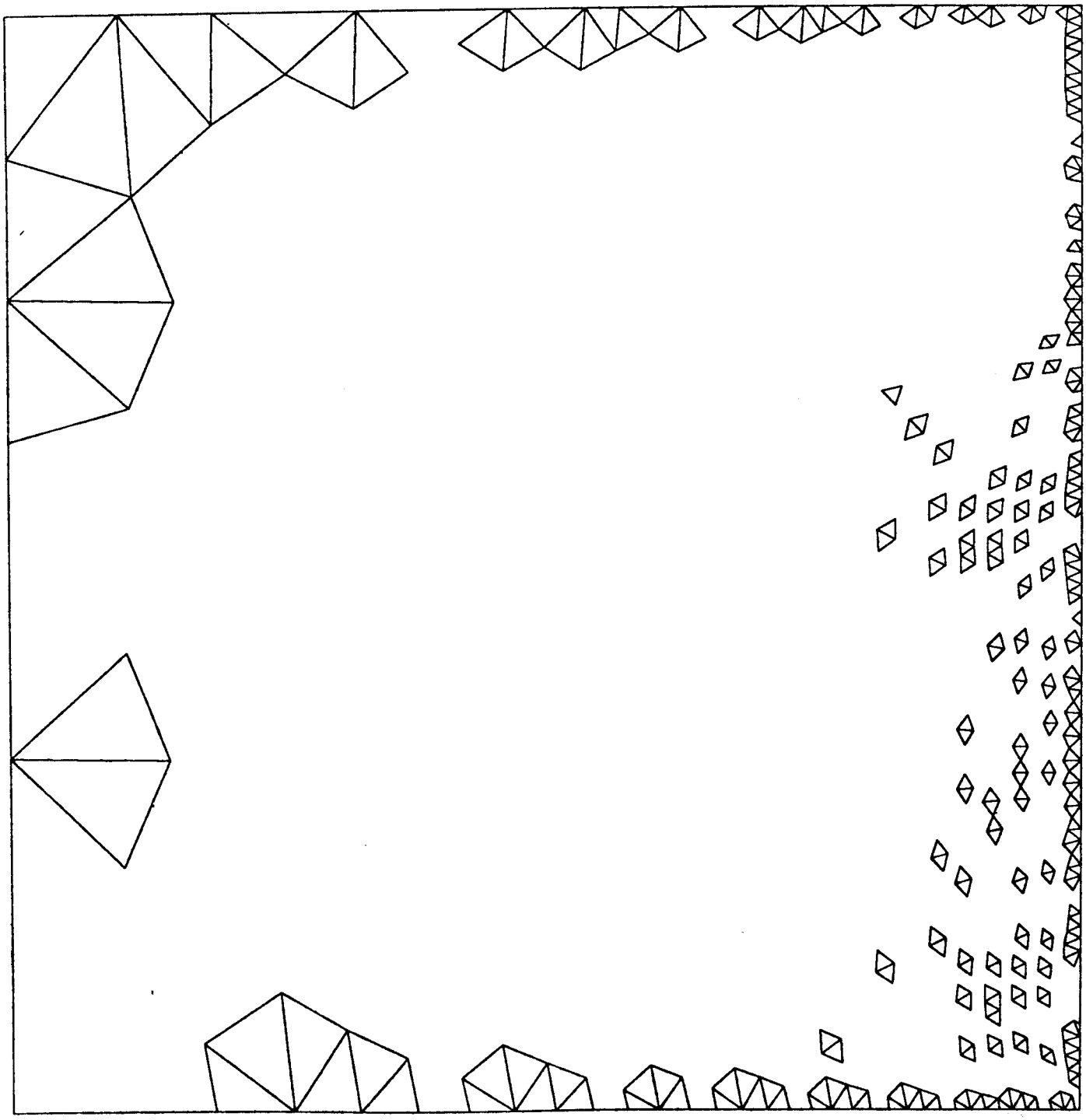

FIG. 11. *Top 10% Error of equilateral triangles for Example 1*

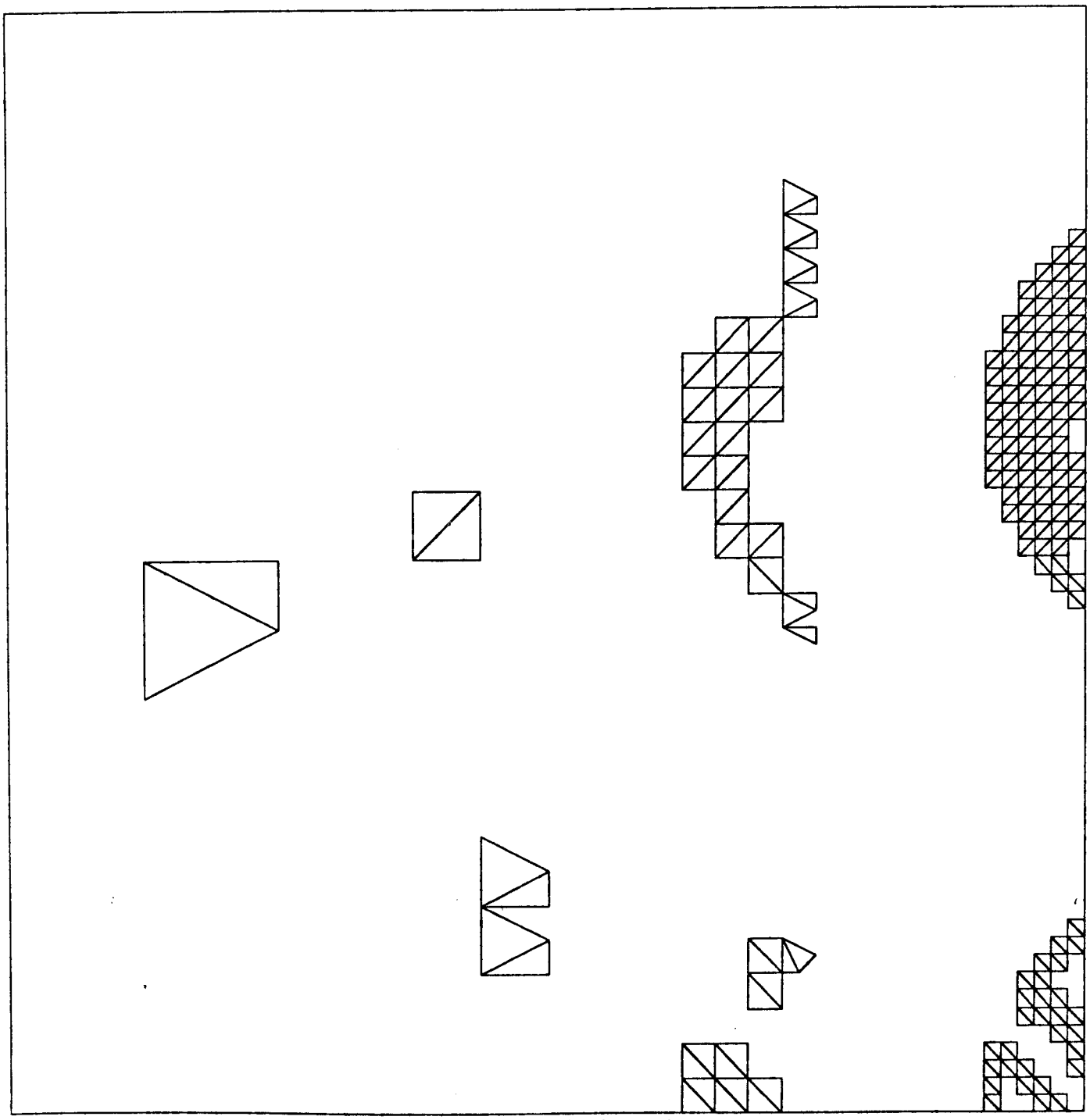

FIG. 12. *Top 10% Error of* PLTMG *for Example 1*

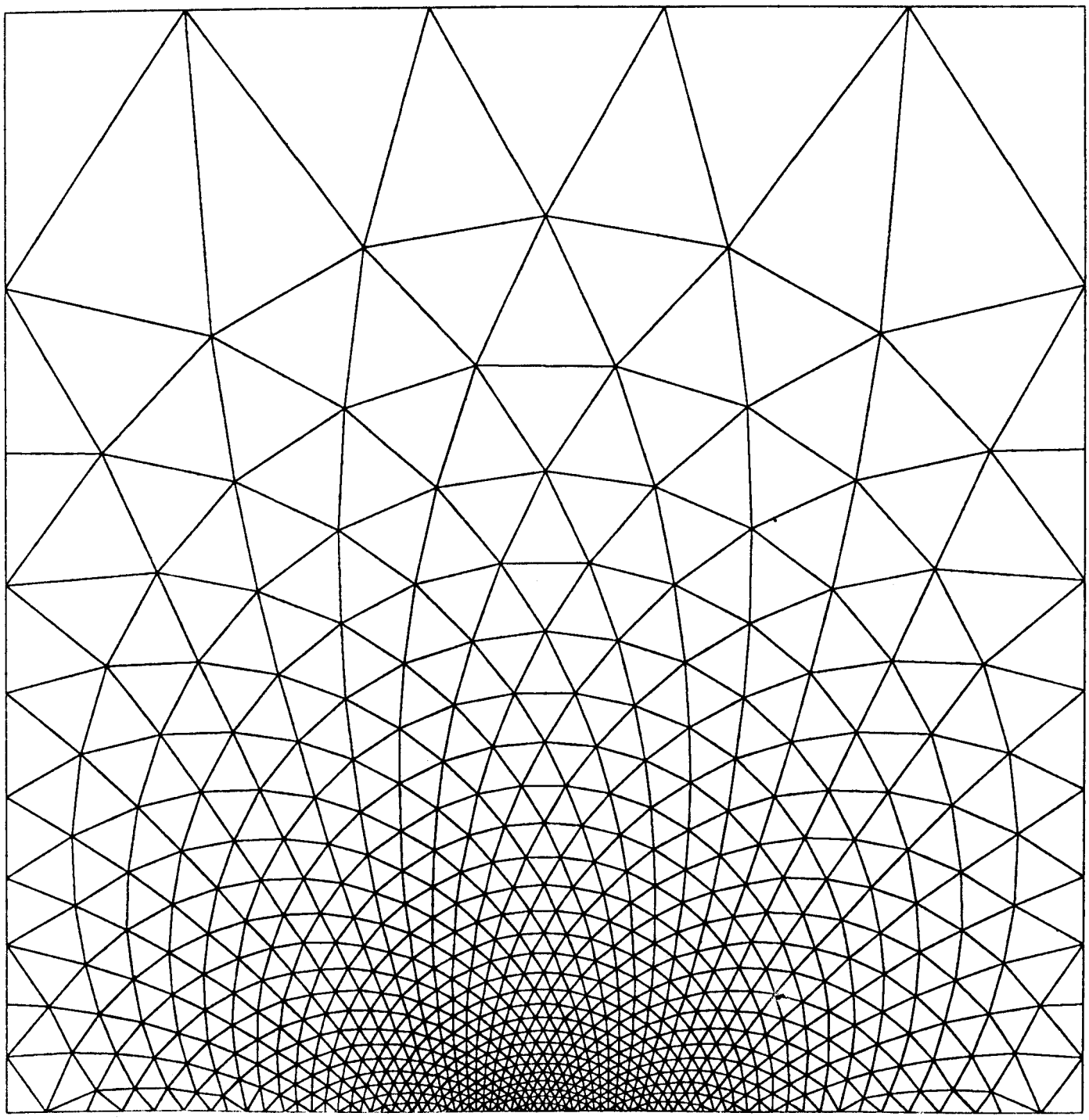

FIG. 13. *Mesh produced by equilateral triangles for Example 2*

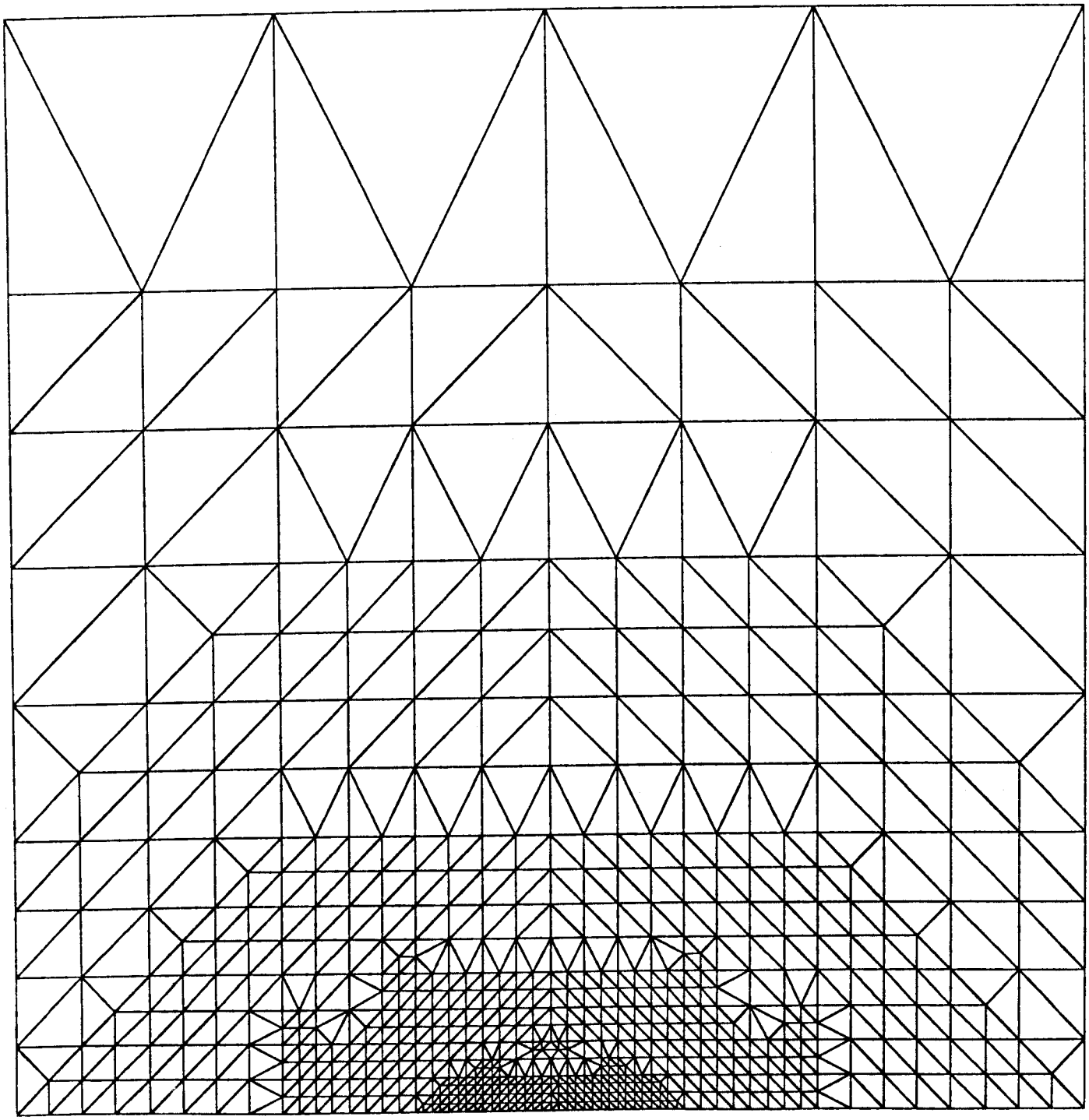

FIG. 14. *Mesh produced by* PLTMG *for Example 2*

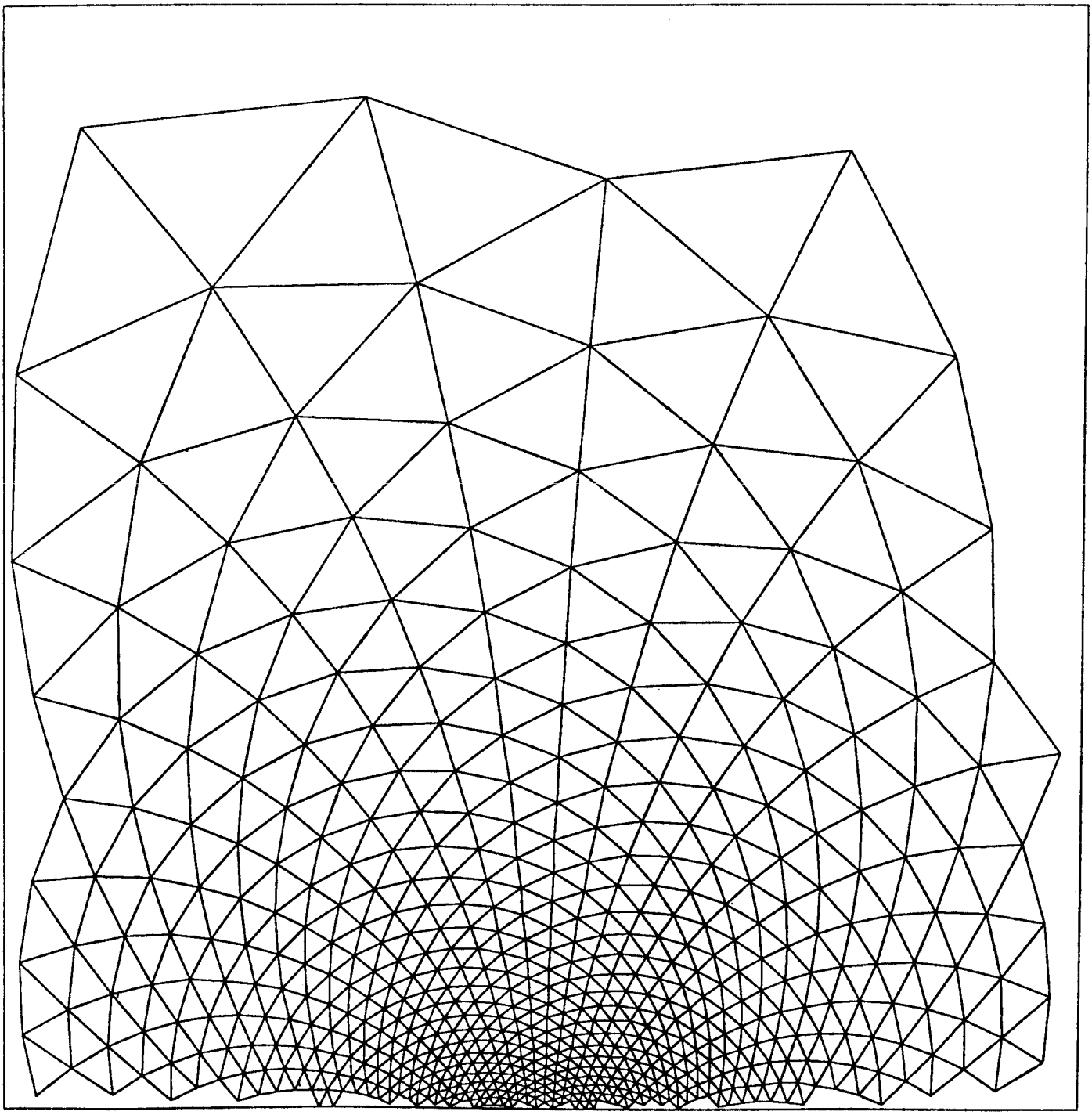

FIG. 15. *Optimally efficient triangulation for Example 2*

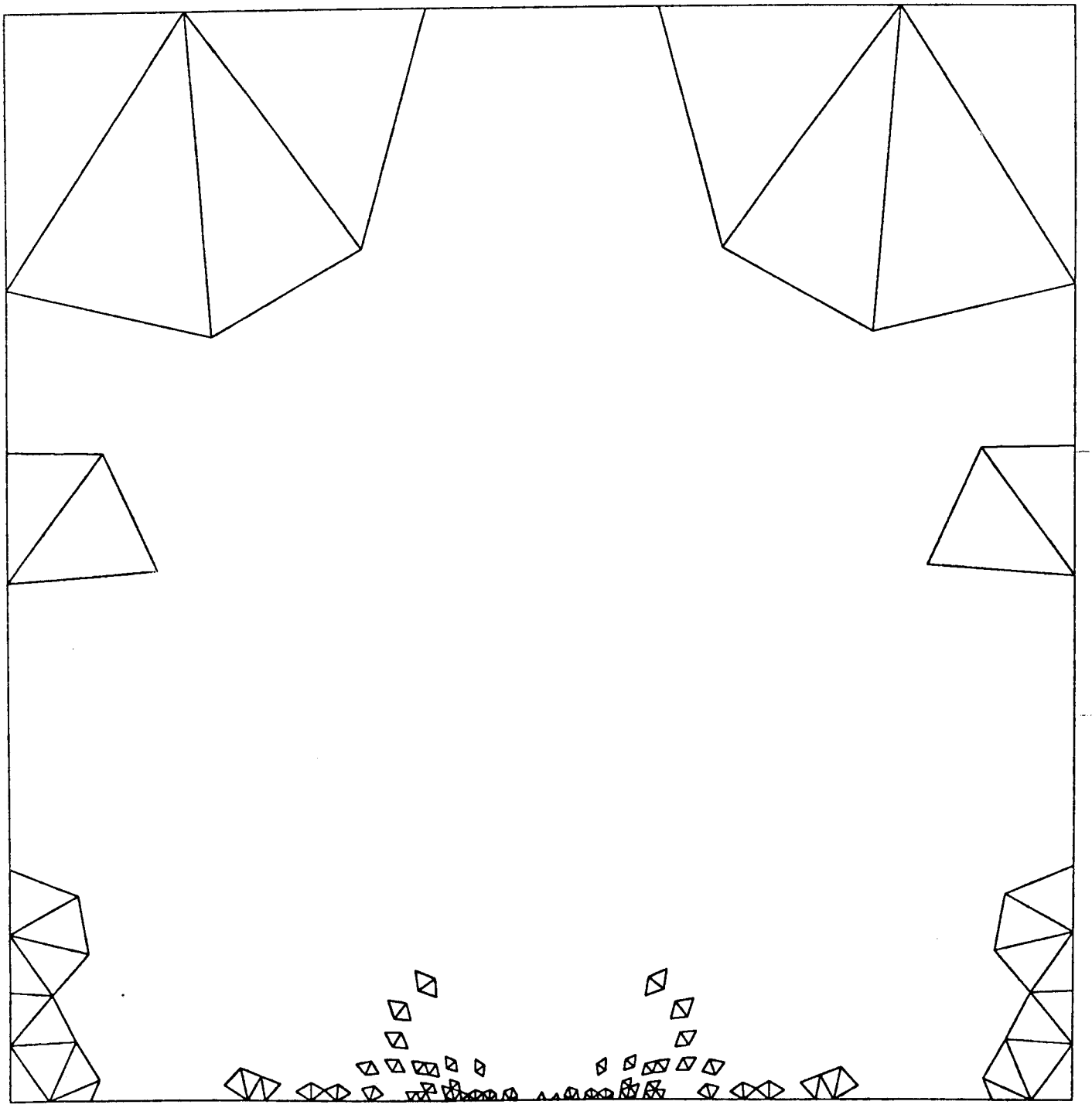

FIG. 16. *Top 10% Error of equilateral triangles for Example 2*

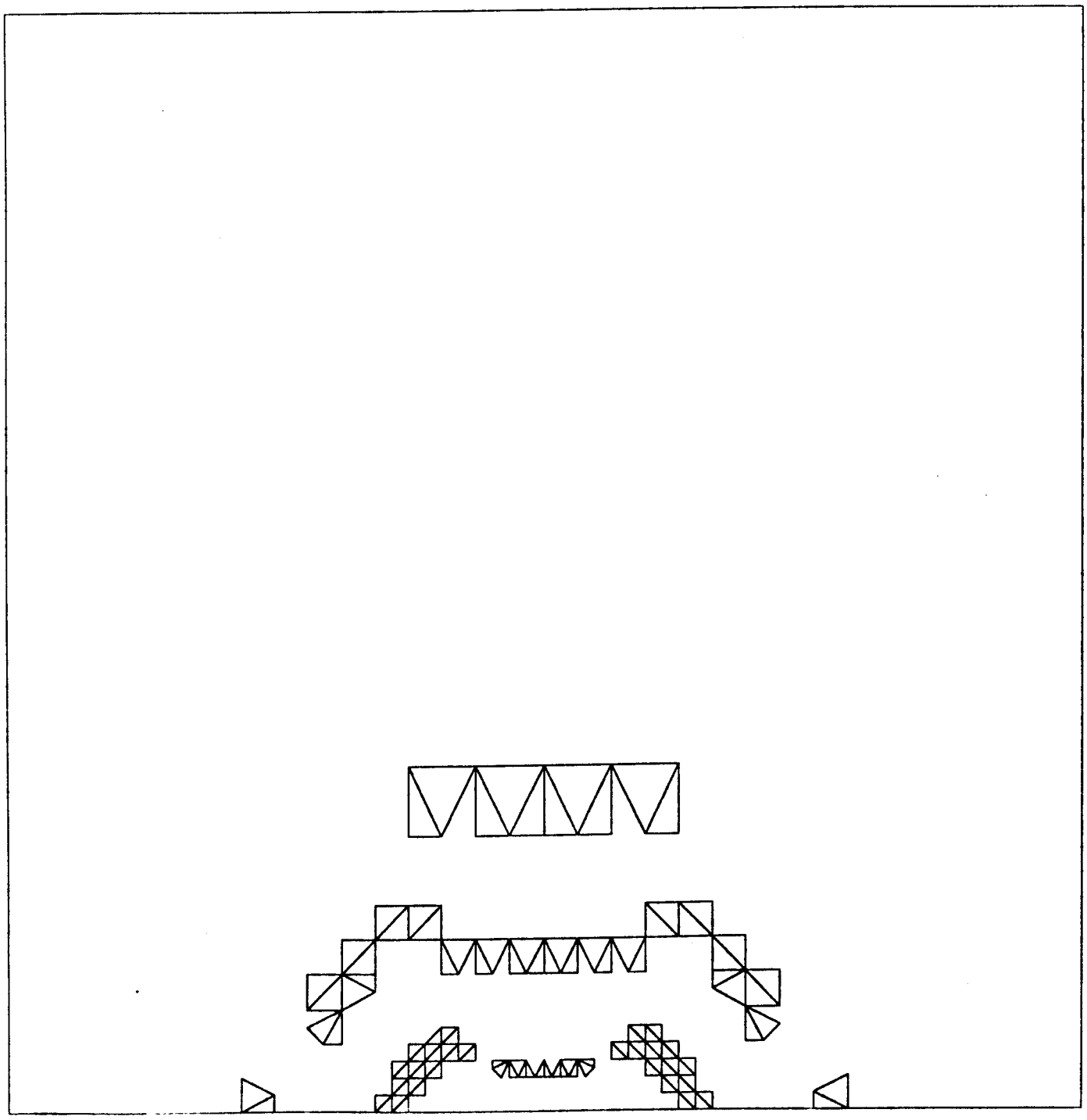

FIG. 17. *Top 10% Error of* PLTMG *for Example 2*

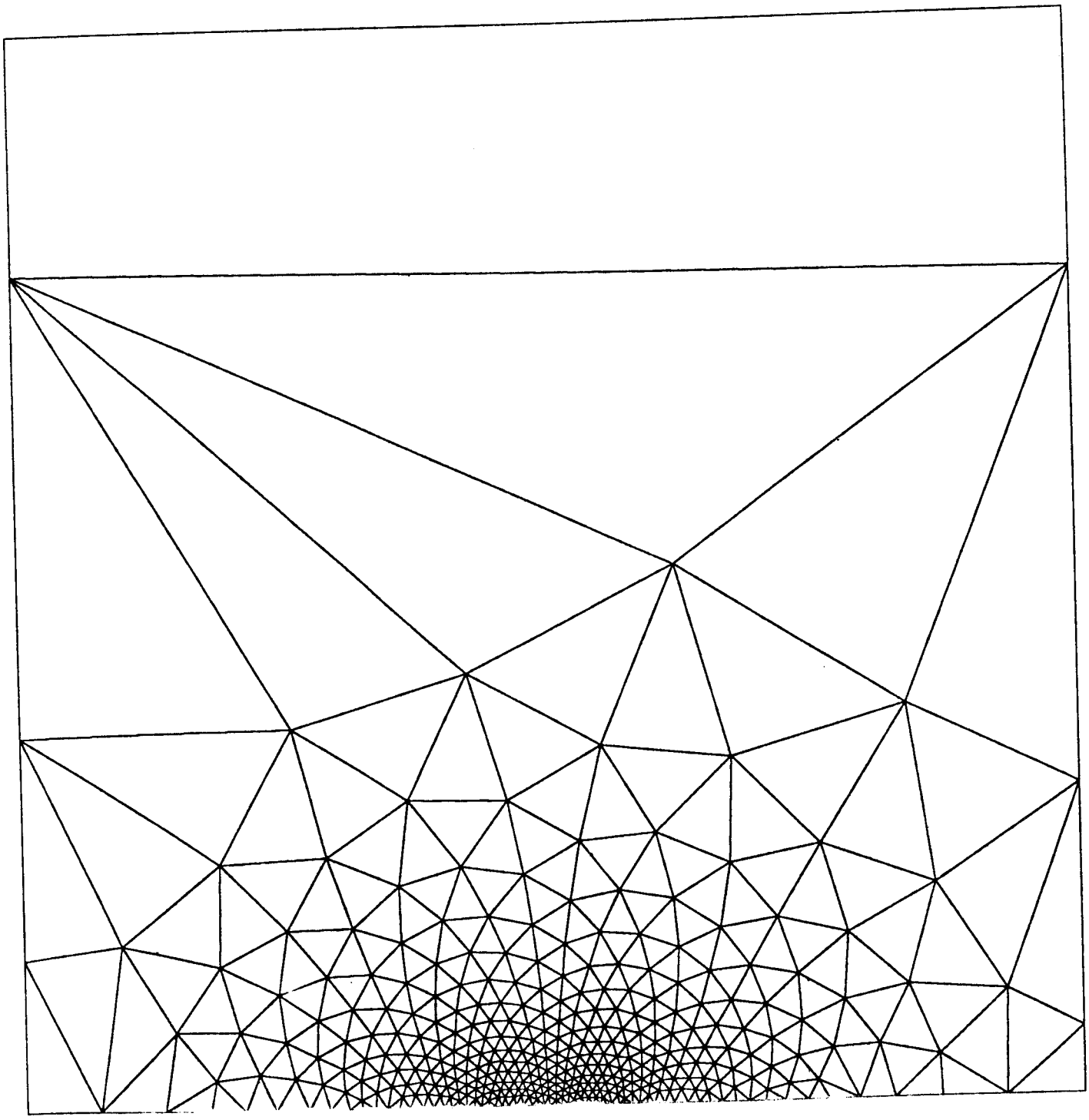

FIG. 18. *Mesh produced by equilateral triangles for Example 3*

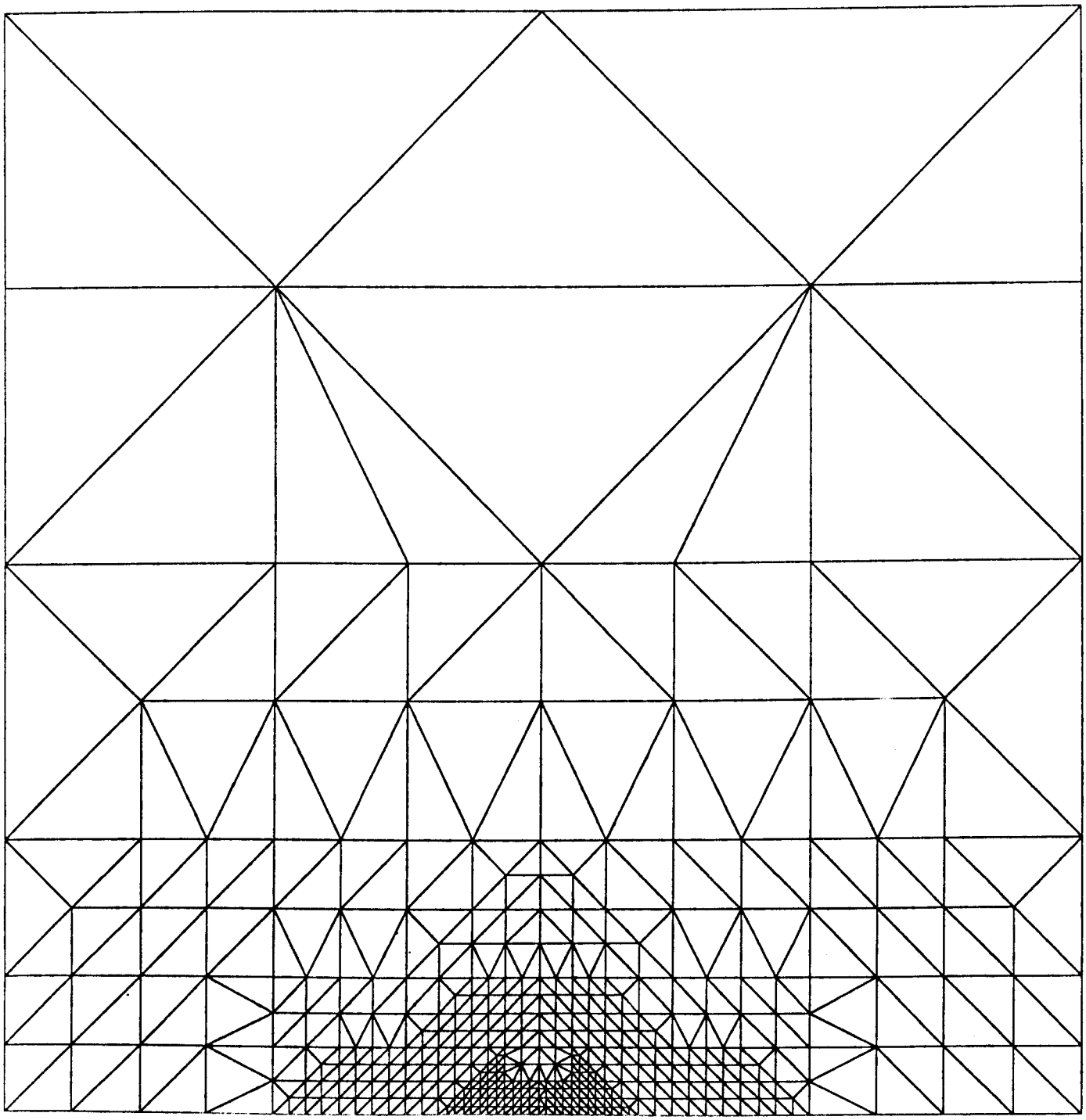

FIG. 19. *Mesh produced by* PLTMG *for Example 3*

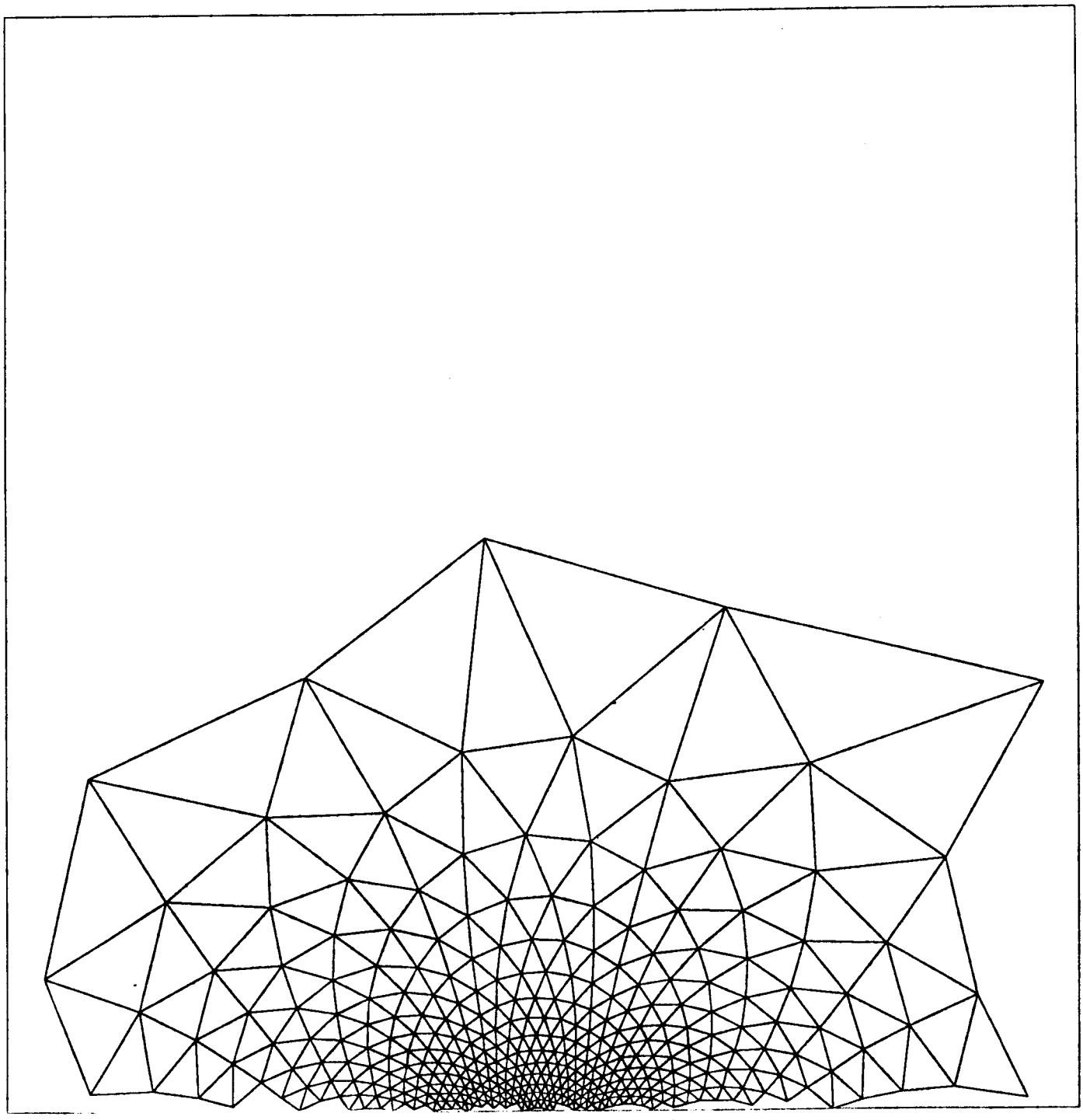

FIG. 20. *Optimally efficient triangulation for Example 3*

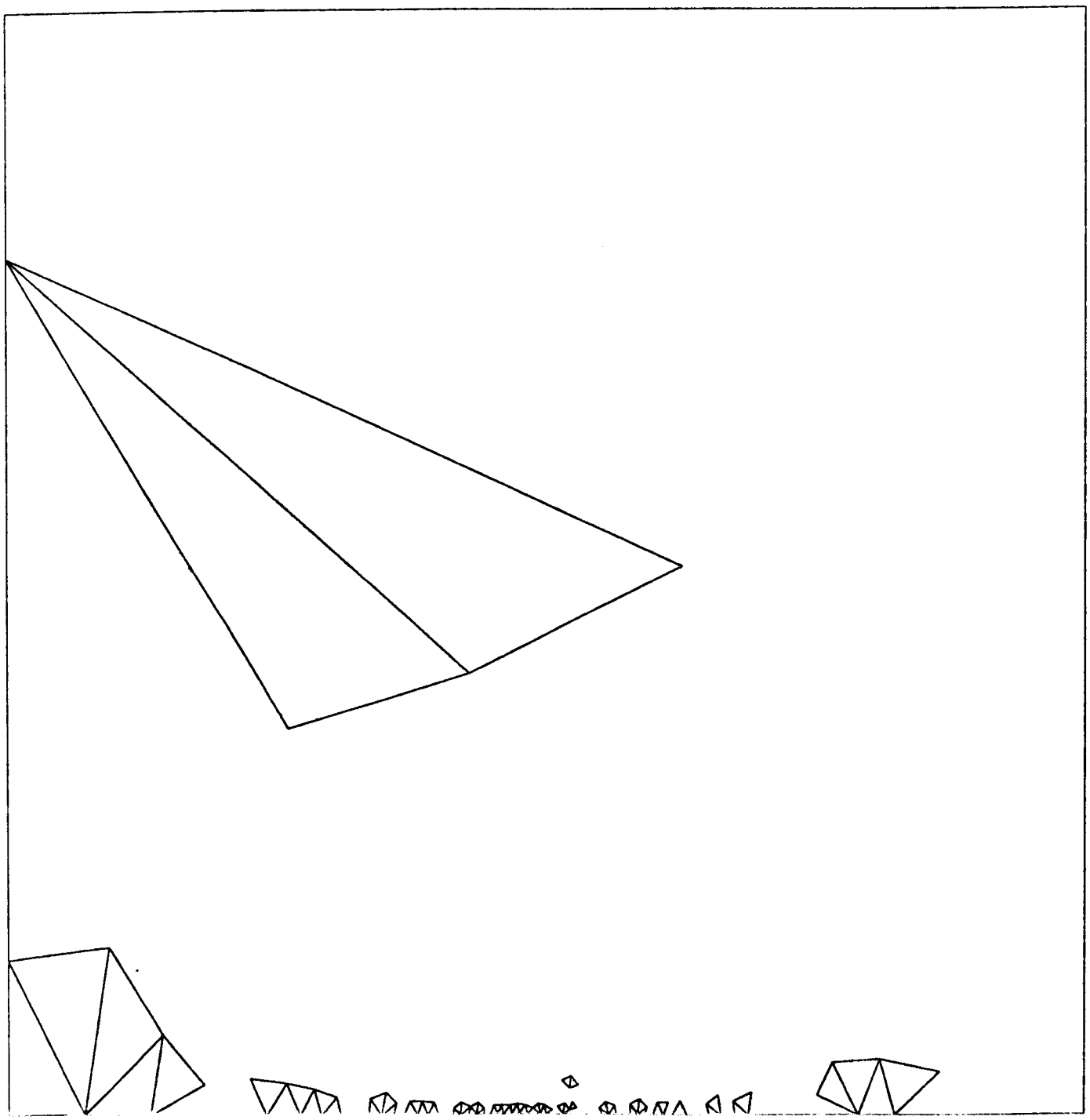

FIG. 21. *Top 10% Error of equilateral triangles for Example 3*

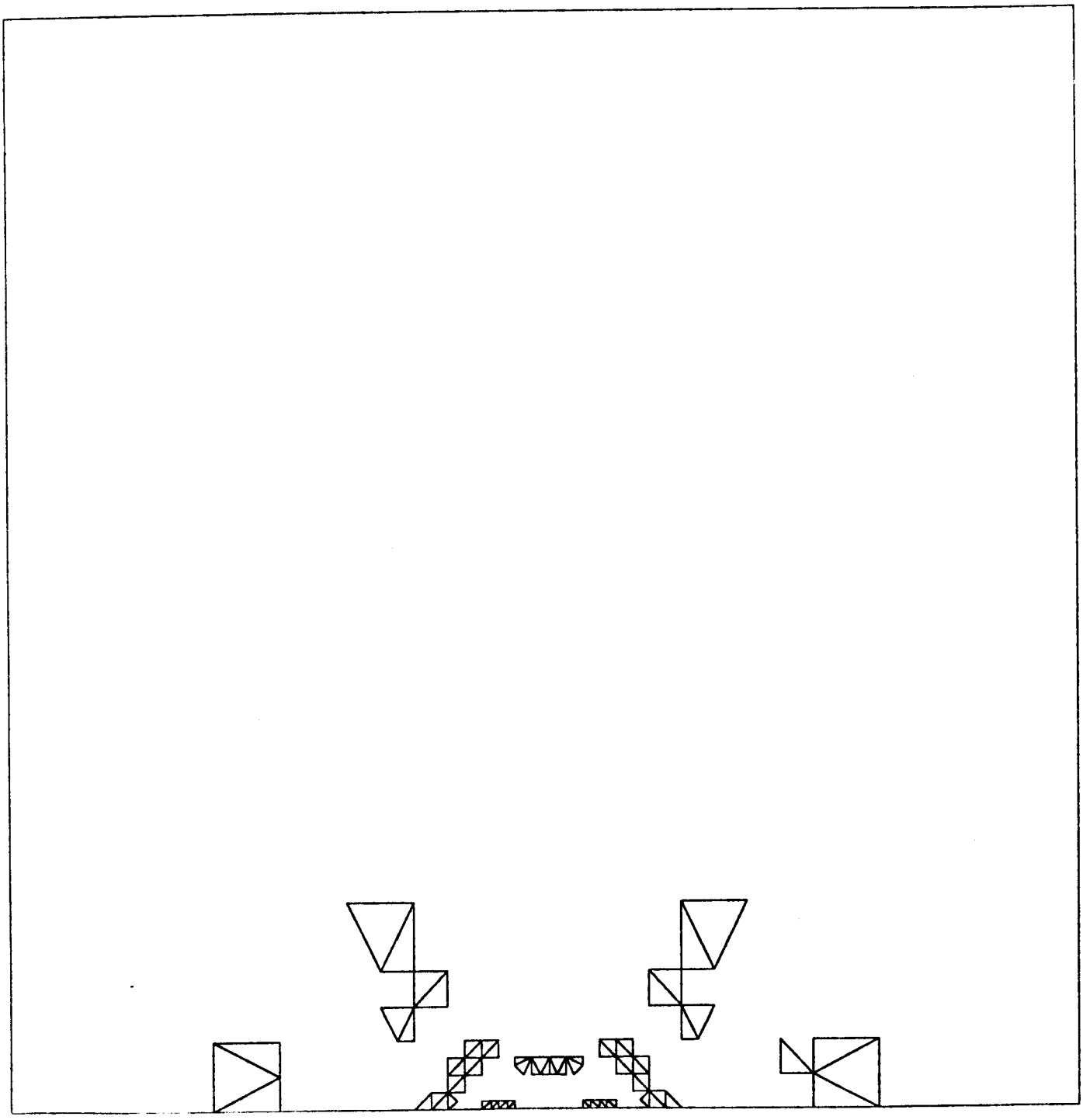

FIG. 22. *Top 10% Error of* PLTMG *for Example 3*

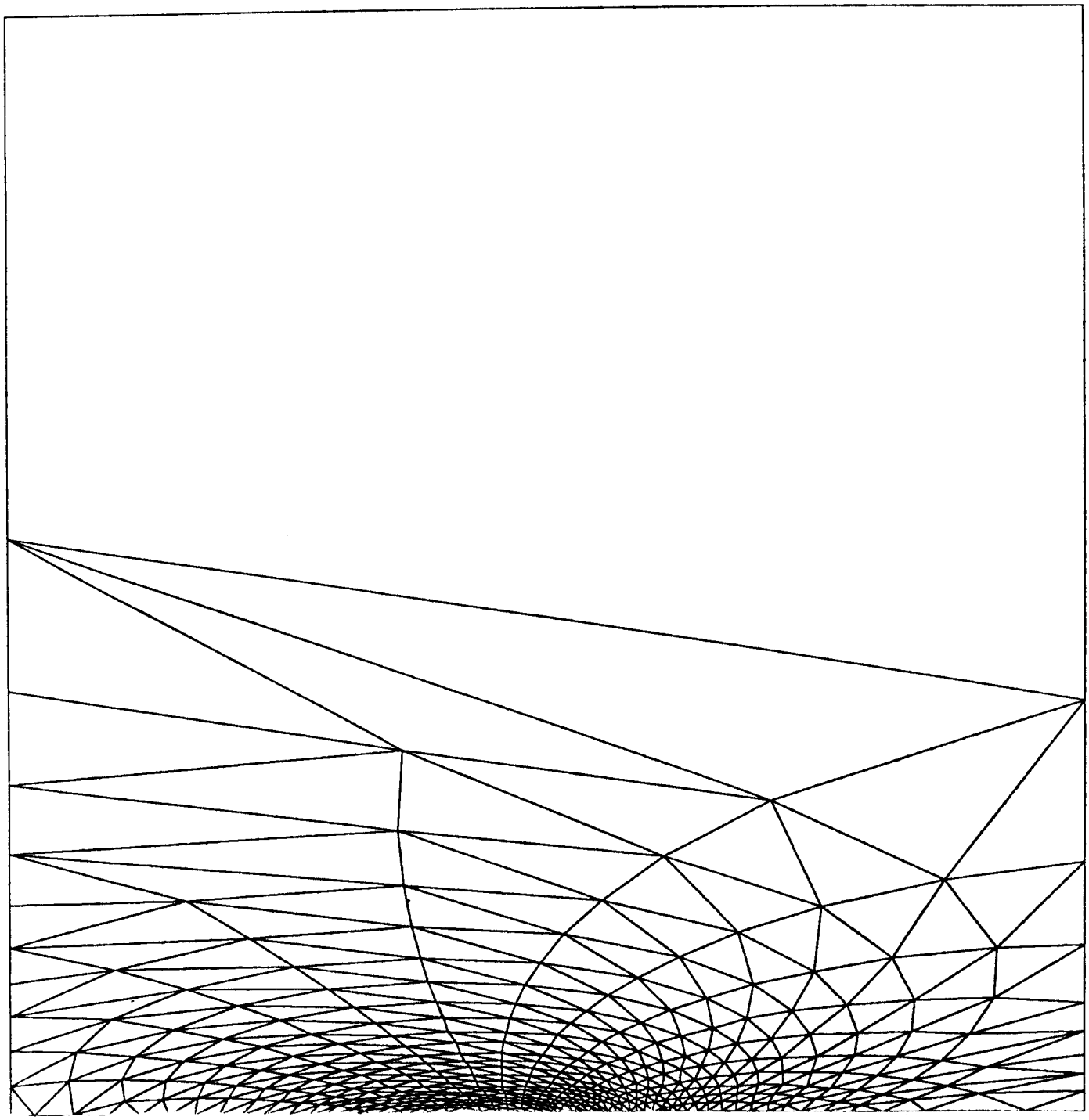

FIG. 23. *Mesh produced by equilateral triangles for Example 4*

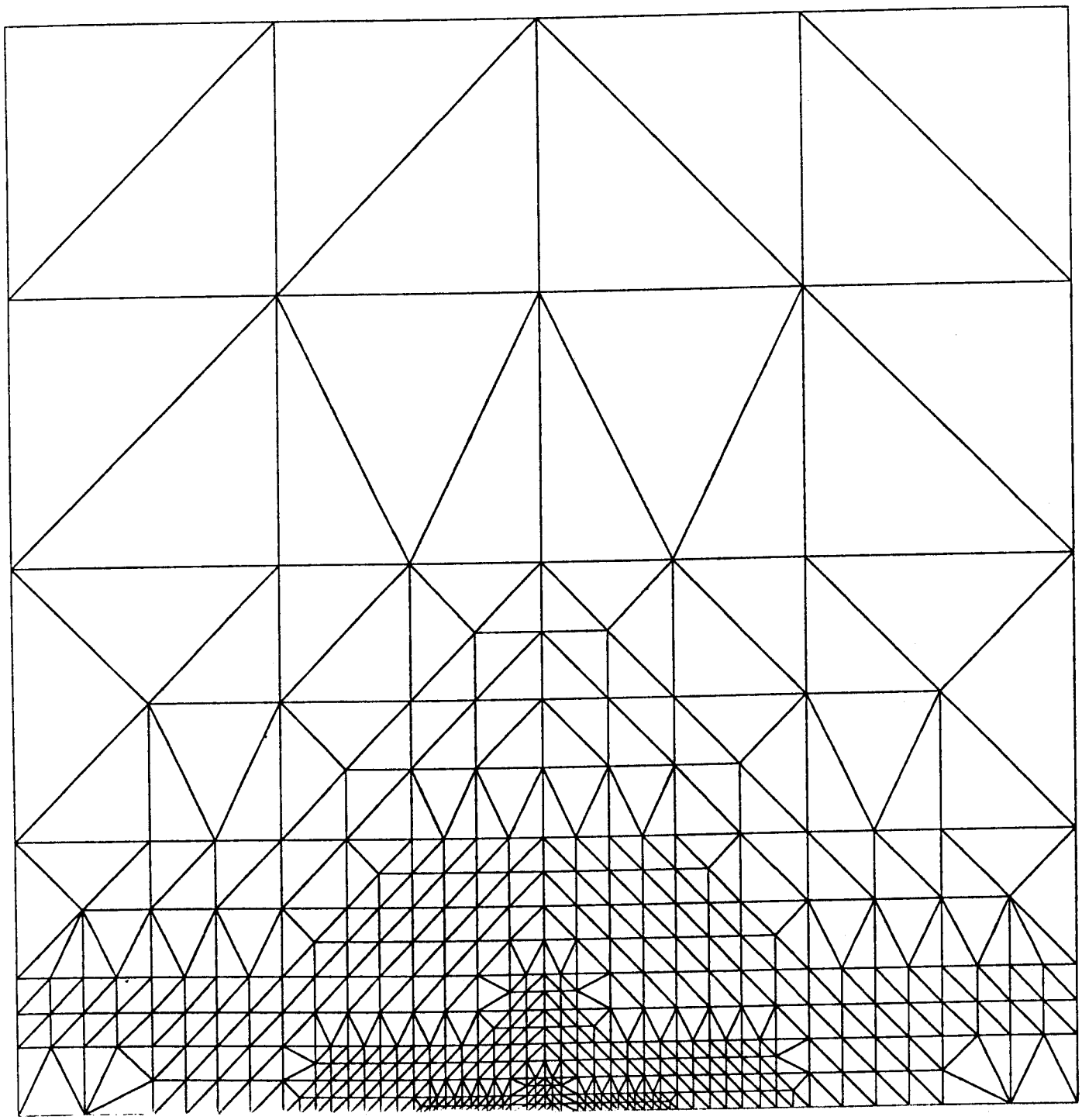

FIG. 24. *Mesh produced by* PLTMG *for Example 4*

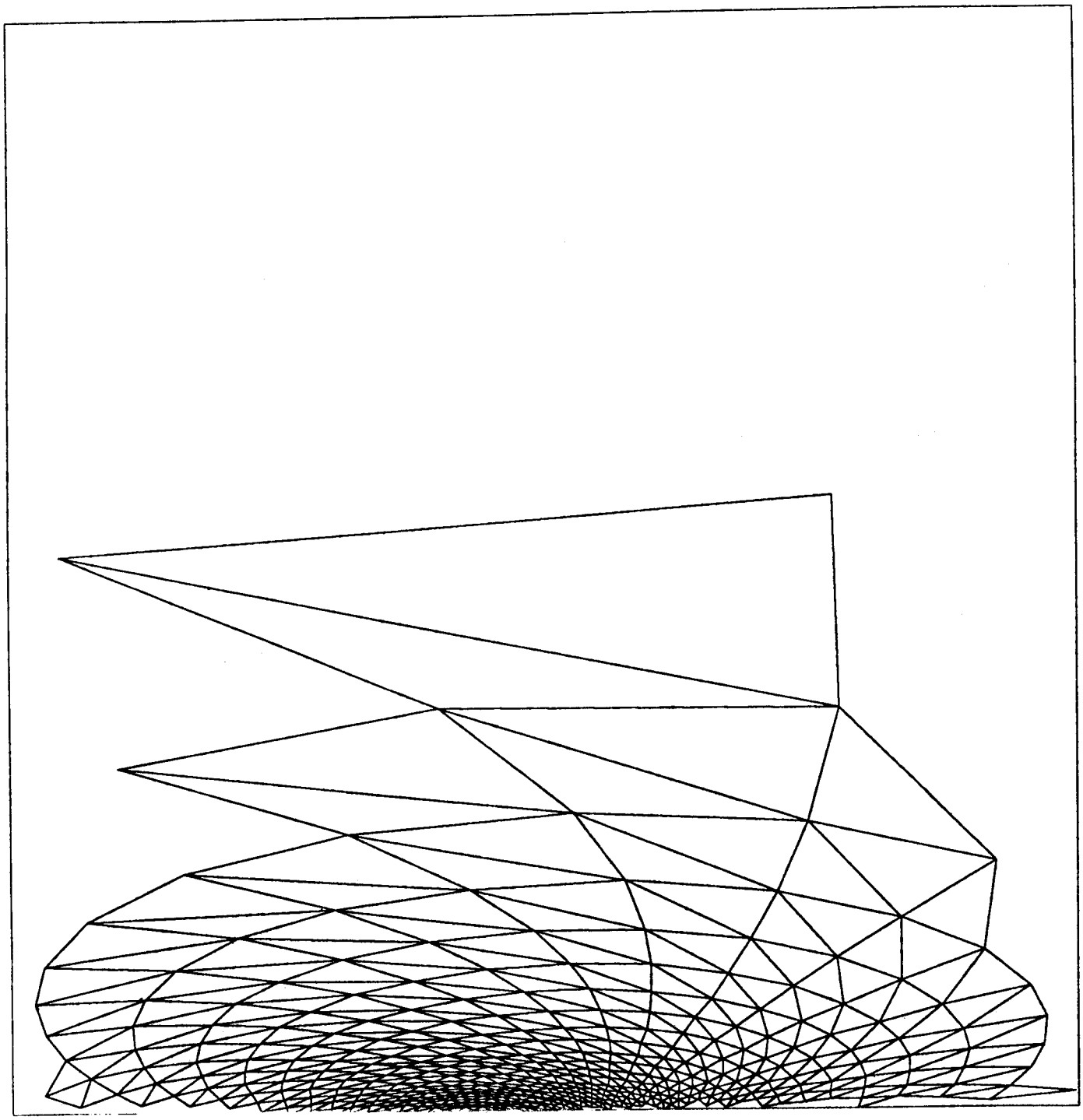

FIG. 25. *Optimally efficient triangulation for Example 4*

REFERENCES

[1] R. E. BANK, PLTMG *user's guide, 1981 version*, tech. rep., Department of Mathematics, University of California at San Diego, August, 1982.

[2] E. F. D'AZEVEDO AND R. B. SIMPSON, *On optimal interpolation triangle incidences*, Research Report CS-88-17, Department of Computer Science, University of Waterloo, Waterloo, Ontario, April, 1988. (to appear in SIAM Journal on Scientific and Statistical Computing).

[3] C. DE BOOR, *Good approximation by splines with variable knots*, in Spline Functions and Approximation Theory, A. Meir and A. Sharma, eds., Springer-Verlag, 1973, pp. 57–71.

[4] M. DELFOUR, G. PAYRE, AND J.-P. ZOLESIO, *An optimal triangulation for second-order elliptic problems*, Computer Methods in Applied Mechanics and Engineering, 50 (1985), pp. 231–261.

[5] A. R. DIAZ, N. KIKUCHI, AND J. E. TAYLOR, *A method of grid optimization for the finite element method*, Computer Methods in Applied Mechanics and Engineering, 41 (1983), pp. 29–45.

[6] C. A. FELIPPA, *Numerical experiments in finite element grid optimization by direct energy search*, Appl. Math. Modelling, 1 (June 1977), pp. 239–244.

[7] ——, *Optimization of finite element grids by direct energy search*, Appl. Math. Modelling, 1 (September 1976), pp. 93–96.

[8] R. LÖHNER, K. MORGAN, AND O. C. ZIENKIEWICZ, *Adaptive grid refinement for the compressible euler equations*, in Accuracy Estimates and Adaptive Refinements in Finite Element Computations, I. Babuska, O. C. Zienkiewicz, J. Gago, and E. R. de A. Oliveira, eds., Wiley-Interscience Publication, 1986, pp. 281–297.

[9] M. B. MCGIRR, D. J. H. CORDEROY, A. K. HELLIER, AND P. C. EASTERBROOK, *The performance of an automatic, self-adaptive finite element technique*, in Computational Techniques & Applications: CTAC-83, J. Noye and C. Fletcher, eds., Elsevier Science Publishers B. V. (North-Holland), 1984, pp. 236–240.

[10] M. B. MCGIRR AND P. KRAUKLIS, *The automatic generation of arrays of nodes with varying density*, in Computational Techniques & Applications: CTAC-83, J. Noye and C. Flectcher, eds., Elsevier Science Publishers B. V. (North-Holland), 1984, pp. 229–235.

[11] E. NADLER, *Piecewise linear best L_2 approximation on triangulations*, in Approximation Theory V, C. K. Chui, L. L. Schumaker, and J. D. Ward, eds., Academic Press, 1986, pp. 499–502. Proceedings of the Fifth International Symposium on Approximation Theory held at Texas A & M University on January 13–17, 1986.

[12] J. PERAIRE, M. VAHDATI, K. MORGAN, AND O. C. ZIENKIEWICZ, *Adaptive remeshing for compressible flow computations*, Journal of Computational Physics, 72 (1987), pp. 449–466.

[13] M. S. SHEPHARD, *Finite element grid optimization — a review*, in Finite Element Grid Optimisation, M. S. Shephard and R. H. Gallagher, eds., The American Society of Mechanical Engineers, June 1979.

[14] M. S. SHEPHARD AND R. H. GALLAGHER, *Finite Element Grid Optimization*, The American Society of Mechanical Engineers, June 1979.

[15] M. S. SHEPHARD, R. H. GALLAGHER, AND J. F. ABEL, *Experience with interactive computer graphics for the synthesis of optimal finite element meshes*, in Finite Element Grid Optimization, M. S. Shephard and R. H. Gallagher, eds., The American Society of Mechanical Engineers, June 1979.

[16] I. S. SOKOLNIKOFF, *Tensor Analysis, Theory and Applications to Geometry and Mechanics of Continua*, John Wiley & Sons, second ed., 1964.

[17] J. L. SYNGE AND A. SCHILD, *Tensor Calculus*, University of Toronto Press, 1949.

[18] J. F. THOMPSON, *Numerical Grid Generation*, North-Holland, 1982. (Also published as Vol. 10, 11 of Applied Mathematics and Computation, 1982).

[19] J. F. THOMPSON, Z. U. A. WARSI, AND C. W. MASTIN, *Numerical Grid Generation: Foundations and Applications*, North-Holland, New York, 1985.

[20] J. F. THOMPSON, Z. U. A. WARSI, AND C. W. MASTIN, *Boundary-fitted coordinate systems for numerical solution of partial differential equations — a review*, Journal of Computational Physics, 47 (July 1982), pp. 1–108.

[21] A. B. WHITE JR., *On selection of equidistributing meshes for two-point boundary-value problems*, SIAM Journal On Numerical Analysis, 16 (June 1979), pp. 472–502.